Review Article

Open Access

Curtis R. Menyuk* and Shaokang Wang

Spectral Methods for Determining the Stability and Noise Performance of Passively Modelocked Lasers

Abstract: We describe spectral or dynamical methods that can be used to determine the stability and noise performance of modelocked lasers. We first review methods that have been used to date to theoretically and computationally study passively modelocked lasers, contrasting evolutionary and dynamical approaches and their application to full, averaged, and reduced models. We then develop the spectral methods and show how they can be used to determine the stability and to calculate the timing jitter and power spectral density for any averaged model with any equilibrium pulse shape. We review work that has been done on soliton lasers using soliton perturbation theory from this dynamical perspective, and we contrast the simplicity and generality of our methods to prior work. We close with a discussion of how to extend our approach from averaged models to full models.

1 Introduction

The most important problem in the modeling of any passively modelocked lasers is usually to find a region in the laser's adjustable parameter space where it operates stably and to optimize the pulse parameters within that region. Adjustable parameters will typically include the cavity length, the pump power, and the amplifier gain, which may be a function of not only the pump power, but also pump wavelength, the material and the geometry of the

*Corresponding Author: Curtis R. Menyuk: Department of Computer Science and Electrical Engineering, University of Maryland, Baltimore County, E-mail: menyuk@umbc.edu
Shaokang Wang: Department of Computer Science and Electrical Engineering, University of Maryland, Baltimore County, E-mail: swan1@umbc.edu

gain media [1]. Typical parameters to be optimized include the pulse energy, the pulse duration, and the pulse timing and phase jitter. Normally, the first should be as large as possible, and the last two should be as small as possible.

These are two basic computational approaches that have been used to model modelocked laser pulses and their stability. With either approach, the first step is to theoretically model the action of the laser components on light as it passes through one roundtrip through the cavity. In the first approach, one iterates the laser model for a large number of roundtrips. If a stationary or periodically stationary solution is obtained at the end of the simulation, it is concluded that a stable modelocked pulse exists. If a stable pulse is not obtained, the opposite is concluded. We refer to this approach as the evolutionary approach. In the second approach, one finds a stationary or periodically-stationary solution (a dynamical equilibrium) either analytically or using a root-finding algorithm. One then linearizes the evolution equations about the equilibrium and examines the spectrum of the linearized equation. If any components of the spectrum have a positive real part, the solution is unstable. We refer to this approach as spectral or dynamical.

These approaches are applied to three types of laser model. In the first type of model, one models the action of each laser component on the light as it passes through the component. We refer to this type of model as full or lumped by analogy to standard electronic circuit terminology. In the second type of model, one averages the action of all the laser components over one roundtrip in the laser. We refer to this type of model as averaged or distributed, again by analogy to electric circuit terminology. In the third type of model, one averages over the pulse shape, only keeping in the model a limited number of pulse parameters, such as its energy, duration, central time, and central phase. We refer to this type of model as reduced.

In Table 1 we summarize the computational approaches and laser model types. We note that both computational approaches can be used in principle with all three

laser model types. However, the dynamical approach has not yet been used with full models.

Table 1: A summary of terminology of laser models and computational approaches that we use throughout this article.

Laser models	full/lumped distributed/averaged reduced
Computational approaches	evolutionary dynamical/spectral

The evolutionary approach to modeling with full laser models mimics the way in which nature generates a mode-locked pulse and is widely used. Its use in laser modeling dates back at least to work by Fox and Li [2] and, for short-pulse lasers, to work by Fleck [3]. This approach is used so extensively that it is not possible to do more than point to a few examples. Siegman [4], Fermann et al. [5], and Kärtner[6] give additional examples. The largest amount of work has been done on lasers that use nonlinear polarization rotation as the saturable absorber mechanism. Soliton fiber lasers have been studied by Chen et al. [7] and Kim et al. [8]. Ilday et al. [9] studied a stretched-pulse fiber laser with a Yb-doped fiber amplifier and optimized its parameters using simulations. Ding et al. [10] used this approach to study a soliton laser that operates with large pulse energies in order to validate a reduced model. Chong et al. [11] and Renninger et al. [12] studied stretched-pulse and similariton lasers that operate in the normal dispersion regime. Spectral filtering plays a critical role in these lasers, and full simulations are useful for optimizing the filter parameters. Baumgartl et al. [13] have used full simulations to study stretched-pulse lasers in the normal dispersion regime and to contrast these lasers to lasers that operate in other regimes.

While nonlinear polarization rotation appears to be the most frequently-used method for obtaining a saturable absorber, nano-scale semiconductor saturable absorber mirrors (SESAMs) have become widely employed for modelocking of not only solid-state lasers, but also for fiber lasers and waveguide lasers. Some examples are GaAs Bragg mirrors [14], nanotubes [15], and graphene saturable absorbers [16]. In nano-scale semiconductor laser diodes, the saturable absorber can also be integrated monolithically in the quantum well/dot structure by electrically isolating one section of the device [17, 18]. The typical design parameters of the saturable absorbers are

the non-saturable loss, the modulation depth, and the response time. When designing a saturable absorber, it is necessary to demonstrate that the absorber can handle high optical powers, short pulse durations, and a wide range of wavelength [19, 20]. Kutz et al. [21] studied lasers that are locked using a SESAM and compared the results of a full model to both an averaged model and experiments. Cabasse et al. [22] carried out full model simulations of a SESAM laser in conjunction with their own experiments.

Full model simulations of solid-state lasers — such as Ti:sapphire lasers — pose a strong challenge to the modeler because the Kerr-lens effect that is the mechanism for the fast saturable absorption is a non-local effect that depends on the lensing of the light within the crystal and the beam's interaction with a mirror that is placed at some distance from the crystal. A full space-time model was developed by Christov and Stoev [23]. They used a relatively simple model for the crystal gain and the frequency dependence of the mirror reflectivity. More recently, Sander et al. [24] studied a 1D model, which replaced the three-dimensional Ti:sapphire crystal with a one-dimensional model based on the nonlinear Schrödinger equation, but kept the full frequency-dependent response of the mirrors and the full cavity dispersion. Renninger and Wise [25] carried out full simulations that predict the existence and stability of pulses in a Ti:sapphire laser that operates in the normal dispersion regime.

An obvious difficulty with full evolutionary models is that they are computationally time-consuming. As a consequence, they are used most often to study existing laser systems and occasionally for single-parameter optimization [11, 12] or to predict the existence of a stable pulse [25], but not to determine the stability boundaries in the parameter space.

In order to speed up the computations, averaged models have been widely used. Features of these models have been reviewed by Kutz [26]. Akhmediev and Ankiewicz [27, 28] provide many examples of how these models may be used. In these models, the effect of the different cavity elements is averaged over one round trip, which leads to a variant of the complex Ginzburg-Landau equation. The most commonly explored equation is the Haus modelocking equation (HME) or master equation, which has been used by Haus and co-workers to model a wide variety of lasers. This work is reviewed in [29]. The most common variant of this equation was first described by Martinez et al. [30], but is based on the original work of Haus [31]. This model relies on the slow saturable gain for stability, but only keeps the cubic nonlinearity in the saturable absorber.

An intermediate approach between an averaged and a full model has recently been described by Lee and Schibli [32], as well as Biondini [33]. In their approach, they treat the periodic variation in one round trip through the laser as a periodic perturbation of an averaged model. In this approach, the periodic variations lead to the generation of continuous waves that act back on the parameters of the modelocked pulse. They compare the results of their evolutionary model to soliton perturbation theory.

Another commonly explored equation is the cubic-quintic Ginzburg-Landau equation (CQGLE), which neglects the slow response of the gain, but keeps the quintic nonlinearity of the saturable absorber. This equation was first investigated in the context of lasers by Moores et al. [34] and Soto-Crespo et al. [35]. The HME has chirped soliton solutions that correspond to a modelocked laser pulse, and their stability has been studied computationally by Kapitula et al. [36], who solved the evolution equations in conjunction with a perturbation analysis. The CQGLE also has analytical pulse solutions, but none of the analytical solutions are stable [35, 37]. However, computational studies of the CQGLE in which the evolution equations are solved has demonstrated the existence of a sizable parameter regime in which stable solutions exist [37, 38]. Leblond et al. [39] have related the parameters of a full vector model of a fiber laser that is locked using nonlinear polarization rotation and then solved the averaged equations to determine the polarizer angles at which the laser operates stably. These results are compared to experiments. The CQGLE effectively models the fast saturable absorber using a Taylor series expansion in the pulse power. Other models of the saturable absorber that have been studied to improve the accuracy of the model are a sinusoidal model [7] and an algebraic model [40].

The HME has also been modified to more accurately replicate the behavior of particular saturable absorbers. Kärtner et al. [41] modeled a SESAM laser in conjunction with a perturbation analysis and experiments. Proctor and Kutz [42] similarly modeled laser modelocking with a waveguide array by solving the evolution equations with a modified version of the HME.

Evolutionary models have rarely been used to study the noise performance of lasers because of the large amount of computer time that is required. However, Pashotta et al. [43, 44] carried out Monte Carlo simulations, solving the HME with amplified spontaneous emission noise in order to verify and extend earlier work by Haus and Mecozzi [45] that used perturbation theory.

Even though the averaged models are far more computationally rapid than full or distributed models, they still run too slowly to have become widely used to carry out broad parameter studies. It is possible to use variational or integral methods in which a pulse shape is assumed — typically a hyperbolic-secant or a Gaussian shape — to reduce the partial differential equation that governs the pulse evolution to a small number of coupled ordinary differential equations that govern the evolution of some number of the pulse parameters such as the pulse's energy, central time, central frequency, central phase, gain, and chirp. As mentioned previously, we refer to models that use this approach as reduced models. While this approach is used most often in conjunction with a perturbative study in which case the equations can be solved analytically, there are cases in which the nonlinear evolution equations are solved. Antonelli et al. [46] used a variational method to derive evolution equations for the pulse energy, pulse duration, chirp, central frequency and central time. They compared the solution of these evolution equations to a solution of the HME and to a perturbative solution. Bale and Kutz [47] use a similar variational approach to derive equations whose solutions they compare to three different averaged models and demonstrate reasonable agreement in all three cases. Kim et al. [8] and Ding and Kutz [10] used this approach to study a laser that is locked using nonlinear polarization rotation. Washburn et al. [48] built on an earlier perturbative model of Newbury and Washburn [49] to study the gain dynamics in a fiber laser. Li et al. [50] built on an earlier perturbative model due to Namiki et al. [51] to study the onset of multi-pulsing.

We now turn to the second computational approach — dynamical or spectral methods.

In this approach, one first finds a stationary or periodically stationary solution of the evolution equations. One then linearizes the evolution equation about this stationary solution, and one obtains a linear equation with constant or periodically varying coefficients. In the case in which the coefficients are constant, the solution of this linearized equation can be decomposed into a sum of modes, each of which varies exponentially in the evolution variable. In the case in which the coefficients are periodic, the linearized equation can again be decomposed into a sum of Floquet-Hill-Bloch modes, each of which varies exponentially in the evolution variable, multiplied by a periodically varying function [52]. If any of the coefficients of the exponential variations — referred to as the spectrum — have a positive real part, then the equilibrium solution is unstable because it is possible for an arbitrarily small perturbation to take the system far away from the equilibrium solution. Conversely, if all the real parts are negative, then any perturbation of the equilibrium solution will decay exponentially. This dynamical approach is one of the mainstays of nonlinear dynamical system theory [53, 54].

Its use in systems that can be described by partial differential equations goes back at least to Maxwell's study of the stability of the rings of Saturn [55]. Once the stability region has been determined, the system can be optimized within its boundaries.

As noted previously, the dynamical approach has not been applied to full models. By contrast, this approach has been extensively applied to averaged models of soliton lasers, and it is only possible to point to a selection of the published work. Haus [29] has applied this approach with his collaborators to study the stability [56] and timing jitter [43] in solid-state lasers, in fiber lasers [57], and in diode lasers [58]. Kärtner et al. [41] extended this approach to lasers that are locked using slow saturable absorbers. Kapitula et al. [36] carried out a careful stability analysis of the HME in which they determined precise stability boundaries. Kutz et al. [21] studied a laser that is locked using a saturable Bragg reflector and Kutz and Sandstede [59] applied this approach to study the stability of a laser that is locked using a waveguide array.

There are many dynamical studies of lasers that use a variational or perturbative approach to determine the stability of a limited number of pulse parameters with a reduced model. Ippen et al. [60] used a perturbative approach to study the stability of additively pulse modelocked lasers. Martinez et al. [30] studied a chirped pulse laser and found conditions for the existence of a pulsed solution. Jirauschek et al. [61] studied Kerr lens modelocking. We have already mentioned work by Bale and Kutz [47], Newbury and Washburn [49], Feng et al. [50], and Namiki et al. [51].

An important limitation of all the dynamical studies that we have cited and all work until very recently is that it is based on an analytically-assumed pulse shape or simple analytical governing equations for the pulse parameters. As a result, the averaged and reduced models cannot be relied upon to be quantitatively accurate over a broad parameter range; the parameters of the averaged model must be carefully determined from experiments or by comparison to a full model. Hence, these models are typically used to give insight into the system behavior and develop qualitative design rules. These models are increasingly suspect even for this purpose. Modern-day passively modelocked lasers are no longer all soliton lasers, but operate in a variety of regimes that in one taxonomy due to Baumgartl et al. [13] have been classified as the soliton, wave-breaking-free, stretched-pulse, chirped-pulse, and ANDi regimes.

It is our view that despite all the work that been done, the current models are inadequate to reliably address the key theoretical issue that we identified at the beginning of this paper — to accurately determine the stability boundaries in the adjustable parameter space of the laser and then optimize its performance. Averaged or reduced models are not sufficiently accurate over a broad parameter range for this purpose.

Full models can be made very accurate, but it is not possible to unambiguously identify the stability boundaries with an evolutionary approach. At a stability boundary, the decay rate for a barely stable solution or the growth rate for a slightly unstable solution becomes zero, and it requires a long evolution time — in principle infinite — to distinguish the two. One can speed the calculation by using a previously-determined equilibrium solution as the starting point for the simulations as one steps through the parameter space, but one must still stop after some amount of evolution time, leading to ambiguities in the result. Moreover, it is possible to fail to capture the perturbations that lead to instability. The large amount of computer time that would be required to carry out this sort of study with a full model, combined with the difficulty just noted is why, to our knowledge, it has not been attempted. While there have been optimization studies using full models [11, 12], these have been done in parameter regimes in which the pulse is highly stable, which limits the computer time that is needed for optimization. However, it is often the case in practice that it is desirable to maximize the pulse energy, minimize the pulse duration, or minimize its timing jitter, which implies operating close to a stability boundary [5, 6].

This difficulty is compounded when studying the response of the laser to input pump noise or amplified spontaneous emission (ASE) noise. In a full evolutionary model, one would naturally be led to doing Monte Carlo simulations, requiring an unfeasibly large amount of computer time. Hence, noise studies in combination with full simulations have not been done. Monte Carlo simulations have been carried out in combination with averaged models [43, 44], but, even in this case, the amount of computer time that is needed is large, and their use is infrequent. We note that the noise level in modern-day lasers is low and treating the noise as a linear perturbation is expected to be highly accurate. As a consequence, it is not necessary to do Monte Carlo simulations. It is sufficient to calculate the means and variances of the quantities of interest. As long as the input noise sources are Gaussian-distributed, as is typically assumed [45], the output distributions will also be Gaussian-distributed.

We have launched a program to address the inadequacies of the current models. The ultimate goal is to combine the accuracy of full models with dynamical methods and advanced computational techniques, so that the models can be reliably used to design modelocked laser systems.

As a first step in this direction, we used dynamical methods to determine the stability of the HME with an additional quintic term in a two-dimensional parameter space [62]. Rather than assume an analytical form for the modelocked pulse (equilibrium solution) or repeatedly determine the shape by solving the evolution equations, as has been done in the past, we treat the determination of this solution as a root-finding problem in a large-dimensional space, which allows us to rapidly find the solution with a good initial guess even near the stability boundaries and also to find unstable equilibria when they exist. Starting from the solution for a known stable equilibrium solution that is obtained by solving the evolution equations, we can then determine the equilibrium as the laser parameters vary by using algorithms that will find solutions regardless of the stability of the solutions. In order to be computationally efficient, we use the stationary solutions that are found for one set of parameters as initial guesses for the root-finding problem for the next set of parameters.

We evaluate the stability by calculating the linearized spectrum in parallel with calculating the stationary solution. We repeat this procedure as parameters vary until we encounter a stability boundary. At that point, we track the boundary. Using this approach, we have shown that it is possible to determine stability boundaries in a two-dimensional parameter space using approximately one hour of computer time on a desktop computer.

The next step of our program is to determine the impact of noise on timing jitter, power spectral density, and other parameters of interest, without assuming an analytical pulse shape for the equilibrium pulse. Much of the work to date on noise impact has been based on soliton perturbation theory [41, 46], which has some peculiarities because the equation that is being perturbed — the nonlinear Schrödinger equation — is a completely integrable mathematical system [63] with no loss or gain. The equations that we will study here, the HME with either a fast or slow saturable loss, are not integrable. Hence, one of our tasks is to recast the problem of determining the quantities of interest into standard spectral terminology.

The remainder of this paper is organized as follows: In Sec. II, we present the equations of interest, and we describe our terminology and methodology. In Sec. III, we apply our methodology to the HME with a fast saturable absorber and compare our results and methodology to those of Haus and Mecozzi [45] and Paschotta [43, 44]. In Sec. IV, we apply our methodology to the HME that has been modified to include a slow saturable absorber, and we compare our results and methodology to those of Kärtner et. al. [41]. In Sec. V, we present our conclusions, combined with a brief discussion of what changes are required to apply our methods to full models, rather than just to averaged models.

2 Our Basic Equations and Methodology

The basic equation that we will be using in our examples is

$$\frac{\partial u}{\partial T} = \left[-i\phi + v\frac{\partial}{\partial t} - \frac{i\beta''}{2}\frac{\partial^2}{\partial t^2} + i\gamma|u|^2 + \frac{g(|u|)}{2}\mathcal{D}_t - \frac{l}{2} + f_{sa}(|u|) \right] u + S(t, T), \quad (1)$$

where $u(t, T)$ is the complex field envelope, t is the retarded fast time, and T is the slow time in the laser, normalized to the average round trip time T_R. The quantity $g(|u|)$ is the slow saturable gain per round trip in the laser, which depends on $|u|^2 = uu^\star$, and in our examples, we will assume that it has the form

$$g(|u|) = \frac{g_0}{1 + P_{av}(|u|)/P_{sat}}, \quad (2)$$

where g_0 is the unsaturated gain, P_{sat} is the saturation power of the amplifier, $P_{av} = (1/T_R) \int_{-T_R/2}^{T_R/2} |u|^2 \, dt$ is the average power in the laser cavity. The operator $\mathcal{D}_t$ is defined as

$$\mathcal{D}_t = \left(1 + i\frac{\omega_{off}}{\omega_g}\frac{\partial}{\partial t} + \frac{1}{2\omega_g^2}\frac{\partial^2}{\partial t^2} \right). \quad (3)$$

The parameters l, β'', and γ are respectively the linear loss, dispersion, and Kerr coefficient per round trip. We are effectively assuming a parabolic gain model whose peak may have an offset with respect to the central frequency ω_{off} and has a gain bandwidth ω_g. In our examples, we will consider two simple models for the saturable absorber. In the first model, we will set $f_{sa}(|u|) = \delta|u|^2$, corresponding to a fast saturable absorber. The quantity δ denotes the strength of the absorber. In the second model, corresponding to a slow saturable absorber, we set $f_{sa}(|u|) = \rho n(t, T)$, where ρ denotes the saturable loss coefficient, and $n(t, T)$ is the fraction of the population in the lower level of a two-level model of the absorber. The quantity $n(t, T)$ is given by the solution to the equation

$$\frac{dn}{dt} = \frac{1 - n}{\tau_A} - \frac{|u|^2}{w_A}n, \quad n(t = -\infty) = 1, \quad (4)$$

where τ_A and w_A denote the response time and saturation energy of the absorber. While we will assume that the absorber is slow compared to the pulse duration, we will also

assume that it is fast compared to the roundtrip time T_R. By contrast, we are assuming that the slow saturable gain is slow compared to T_R.

The quantities ϕ and ν represent a phase shift and a time shift per round trip. It is conventional in analytical studies of modelocking to set these quantities to zero. In that case, there is no steady-state or equilibrium solution to Eq. (1) for most choices of the parameters, and one searches for a solution to this equation with a steady phase rotation and/or drift. This approach is not consistent with standard dynamical methods, which require a true equilibrium, and does not generalize well to computational studies, where it is desirable to set the left side of Eq. (1) equal to zero and use root-finding methods to find the equilibrium [62]. Thus, we leave ϕ and ν as unknown parameters that are determined as part of the process of finding an equilibrium solution $[\phi_0, \nu_0, u_0(t)]$. From a physical standpoint, setting ν and ϕ equal to zero corresponds to nulling the linear group and phase velocities, while our choice corresponds to nulling the velocity and phase change of the modelocked pulse.

The statistical behavior of the noise in our examples is governed by

$$\begin{aligned}\left\langle S(t, T)S(t', T')\right\rangle &= \left\langle S^\star(t, T)S^\star(t', T')\right\rangle = 0, \\ \left\langle S(t, T)S^\star(t', T')\right\rangle &= D\delta(t - t')\delta(T - T'),\end{aligned} \tag{5}$$

where the brackets indicate an ensemble average, and we are effectively assuming that the noise is white. The dynamical method that we will outline is still applicable with more general noise assumptions, in which the noise will not necessarily be Gaussian distributed, but we must assume that the noise is perturbative and does not affect the equilibrium solution. Indeed, without this assumption, there is no equilibrium solution, and the dynamical methods that we will present here cannot be applied without large modifications.

We will assume that any quantity of interest can be expressed as the inner product of a fixed vector with the noise perturbation in an appropriate Hilbert space, and we will shortly give several examples. As our starting point, we must define an appropriate Hilbert space and inner product [64]. Any equation for the evolution of $u(t, T)$ involves both $u(t, T)$ and $u^\star(t, T)$. That is a consequence of the slowly varying envelope approximation and the presence of nonlinearity. Hence, perturbations of u and $u^\star$ must be treated independently [65]. The modes $[\Delta u, \Delta \bar{u}]$ of the linearized equation corresponding to an equilibrium solution $[u_0, u_0^\star]$ do not generally come in complex conjugate pairs. For this reason, it is useful to define vectors $\mathbf{f}(t) = [f(t), \bar{f}(t)]^T$, where, again, the variable $\bar{f}$ is not necessarily the complex conjugate of f, and the superscript T

indicates a transpose, so that $\mathbf{f}$ can be viewed as a two-element column vector that is a function of t. Two vectors in the Hilbert space have the inner product

$$[\![\mathbf{f}|\mathbf{h}]\!] = \int\limits_{-\infty}^{\infty} dt \left[f^\star(t)h(t) + \bar{f}^\star(t)\bar{h}(t) \right]. \tag{6}$$

We will often be interested in cases for which $\bar{f}(t) = f^\star(t)$ and $\bar{h}(t) = h^\star(t)$. In that case, we find

$$[\![\mathbf{f}|\mathbf{h}]\!] = 2\,\mathrm{Re}\left[\int\limits_{-\infty}^{\infty} dt\, f^\star(t)h(t) \right]. \tag{7}$$

In the examples that we will consider here, we define the functional derivatives $DF(u, \bar{u})/Du$ and $DF(u, \bar{u})/D\bar{u}$ using the Fréchet derivative [66]. Suppose $u(t, T) = u_0(t) + \epsilon\Delta u(t, T)$ and $\bar{u}(t, T) = u_0^\star(t) + \epsilon\Delta\bar{u}(t, T)$, then the Fréchet derivatives of $F(u, \bar{u})$ are defined via the relations

$$\begin{aligned}\left.\frac{DF(u, \bar{u})}{Du}\right|_{u=u_0, \bar{u}=u_0^\star} &\cdot \Delta u = \\ &\lim_{\epsilon \to 0}\left[F\left(u_0 + \epsilon\Delta u, u_0^\star\right) - F(u_0, u_0^\star) \right]/\epsilon, \\ \left.\frac{DF(u, \bar{u})}{D\bar{u}}\right|_{u=u_0, \bar{u}=u_0^\star} &\cdot \Delta\bar{u} = \\ &\lim_{\epsilon \to 0}\left[F\left(u_0, u_0^\star + \epsilon\Delta\bar{u}\right) - F(u_0, u_0^\star) \right]/\epsilon.\end{aligned} \tag{8}$$

where we stress that u and $\bar{u}$ are treated as independent variables. We use the central dot here to indicate that the function derivatives in general act as operators that involve integrals over Δu and $\Delta\bar{u}$. For example, given the slow saturable gain $g(|u|) \equiv g(u, \bar{u})$ as defined in Eq. (2) with $\bar{u} = u^\star$, we find

$$\left.\frac{Dg}{Du}\right|_{u=u_0, \bar{u}=u_0^\star} \cdot \Delta u = -\frac{[g(|u_0|)]^2}{g_0 T_R P_{\mathrm{sat}}} \int\limits_{-\infty}^{\infty} dt \left[u_0^\star(t)\Delta u(t) \right]. \tag{9}$$

In this paper, the functional derivatives will always be evaluated at $u = u_0$ and $\bar{u} = u_0^\star$; so, henceforward, we will not explicitly note this. Because u and $\bar{u}$ must be treated as independent when evaluating the functional derivatives, the first step in obtaining Eq. (9) is to write Eq. (2) in the form $g(|u|) \equiv g(u, \bar{u}) = g_0 \left[1 + P_{\mathrm{av}}(u, \bar{u})/P_{\mathrm{sat}} \right]^{-1}$ with $P_{\mathrm{av}} = (1/T_R)\int_{-T_R/2}^{T_R/2} u(t)\bar{u}(t)dt$, so that $[DP_{\mathrm{av}}(u, \bar{u})/Du] \cdot \Delta u$ becomes $(1/T_R)\int_{-T_R/2}^{T_R/2} u_0^\star\Delta u dt$, from which Eq. (9) follows.

We can now write Eq. (1) and the functional derivatives to find the derivatives of Δu and $\Delta\bar{u}$ with respect to the slow time T. If we write $\partial u/\partial T = F(|u|) \equiv F(u, \bar{u})$, it follows that

$$\frac{\partial\Delta u}{\partial T} = \frac{DF}{Du} \cdot \Delta u + \frac{DF}{D\bar{u}} \cdot \Delta\bar{u}, \tag{10}$$

which can be further written as

$$\frac{\partial \Delta u}{\partial T} = \left[-i\phi + \nu \frac{\partial}{\partial t} + \frac{g(|u_0|)}{2}\mathcal{D}_t - \frac{l}{2} - \frac{i\beta''}{2}\frac{\partial^2}{\partial t^2} \right.$$
$$\left. + 2i\gamma|u_0|^2 + f_{sa}(|u_0|) \right] \Delta u + i\gamma u_0^2 \Delta\bar{u}$$
$$+ u_0 \left[\frac{Df_{sa}}{Du} \cdot \Delta u + \frac{Df_{sa}}{D\bar{u}} \cdot \Delta\bar{u} \right]$$
$$+ \frac{1}{2}\left[\frac{Dg}{Du} \cdot \Delta u + \frac{Dg}{D\bar{u}} \cdot \Delta\bar{u} \right]\mathcal{D}_t u_0, \qquad (11)$$

and a similar equation can be obtained for $\partial\Delta\bar{u}/\partial T$. This equation can be obtained most easily by taking the complex conjugate of Eq. (11) and replacing $\Delta\bar{u}^*$ with Δu and Δu^* with $\Delta\bar{u}$. This simple transformation yields the correct answer because the equation governing u_0^* is the complex conjugate of Eq. (1), and all functional derivatives are evaluated at $u = u_0$ and $\bar{u} = u_0^*$. As a consequence, if Δu and $\Delta\bar{u}$ are complex conjugates at any time T, then they are complex conjugates at all times T.

Explicit expressions for the functional derivatives of $g(|u|)$ and $f_{sa}(|u|)$ are given for example in [41, 46, 62]. We have already given the expansion for $[Dg/Du] \cdot \Delta u$ in Eq. (9), and we can obtain the expression for $[Dg/D\bar{u}] \cdot \Delta\bar{u}$ in a similar fashion. For the fast saturable absorber, we have simply $(Df_{sa}/Du) \cdot \Delta u = \delta u_0^* \Delta u$, which is a local operation in the fast time. However, Eq. (4) implies that $f_{sa}(|u|) = \rho n(t, T)$ is a non-local functional of u since its value at any time t depends on u at earlier times. Hence, its functional derivatives will also be non-local. The calculation in this case is more complicated. From Eq. (4), we find

$$\frac{d}{dt}\frac{Df_{sa}}{Du} = -\rho \left[\frac{1}{\tau_A} + \frac{|u_0(t)|^2}{\omega_A} \right]\frac{Dn}{Du} - \frac{\rho u_0^*}{\omega_A}n(|u_0|), \quad (12)$$

where n can be obtained by integration of Eq. (4),

$$n(|u|) = \exp\left[\frac{w(t_0) - w(t)}{w_A} + \frac{t_0 - t}{\tau_A} \right]$$
$$+ \frac{1}{\tau_A}\int_{t_0}^{t} dt' \exp\left[\frac{t' - t}{\tau_A} + \frac{w(t') - w(t)}{w_A} \right], \qquad (13)$$

with $w(t) = \int_{-\infty}^{t}|u(t')|^2 dt'$. Integrating Eq. (12) will yield $[Df_{sa}/Du](t)$. Multiplying by $\Delta u(t)$ and integrating over t will yield $[Df_{sa}/Du] \cdot \Delta u$.

We note parenthetically that it is more computationally efficient to use $\Delta v = (\Delta u + \Delta\bar{u})/2$ and $\Delta w = (\Delta u - \Delta\bar{u})/2i$ in place of of Δu and $\Delta\bar{u}$ since both Δv and Δw are real when $\Delta u^* = \Delta\bar{u}$ [62]. We will not discuss this formulation further here since it complicates the comparison to the earlier analytical work of Haus and Mecozzi [45] and Kärtner

et al. [41]. However, we do use it when obtaining computational results.

We now give three examples in which a quantity of interest is expressed as an inner product.

Example 1: A parameter of critical importance in applications is the timing jitter. It is usually desirable to make it as small as possible. The fundamental definition of the central time is

$$t_c = \frac{\int_{-\infty}^{\infty} t|u(t, T)|^2 dt}{\int_{-\infty}^{\infty} |u(t, T)|^2 dt}. \qquad (14)$$

If we choose the central time of the equilibrium pulse to be at $t = 0$, then we find that the change in the central time t_c due to a perturbation becomes

$$\Delta t_c = \frac{1}{w_0}\int_{-\infty}^{\infty} t\left[u_0^*(t, T)\Delta u(t, T) + u_0(t, T)\Delta u^*(t, T) \right]dt, \qquad (15)$$

where $w_0 = \int_{-\infty}^{\infty}|u_0|^2 dt$. If we let $f_c = tu_0/w_0$, $\bar{f}_c = tu_0^*/w_0$, and $\Delta\bar{u} = \Delta u^*$, we see that

$$\Delta t_c = [\![\mathbf{f}_c | \Delta\mathbf{u}]\!], \qquad (16)$$

where $\mathbf{f}_c = [f_c, f_c^*]^T$. The variance of the timing jitter is given by

$$\langle \Delta t_c^2 \rangle = \langle [\![\mathbf{f}_c | \Delta\mathbf{u}]\!]^2 \rangle. \qquad (17)$$

Example 2: In experiments, it is usual to measure the power spectral density of the phase noise as a function of frequency f that is produced by a photodetector, $S_\phi(f)$. As shown for example by Paschotta [43], we may write $S_\phi(f) = (1/f^2)S_{frep}$, where

$$S_{frep}(f) = \int_{-\infty}^{\infty} dT' \exp(2\pi i fT')\langle [\Delta t_c(T) - \Delta t_c(T - 1)]$$
$$\times [\Delta t_c(T + T') - \Delta t_c(T + T' - 1)]\rangle$$
$$\simeq \int_{-\infty}^{\infty} dT' \exp(2\pi i fT')\langle \Delta t_c'(T)\Delta t_c'(T + T') \rangle, \quad (18)$$

where $\Delta t_c' = d\Delta t_c/dT$. We write

$$\frac{\partial \Delta\mathbf{u}}{\partial T} = \mathsf{L}\Delta\mathbf{u} + \mathbf{S(t, T)}, \qquad (19)$$

where the operator L is given by Eq. (11) and the corresponding equation for $\Delta\bar{u}$, and we define $\mathbf{S} = [S, S^*]^T$. We now find

$$S_{frep} = \int_{-\infty}^{\infty} dT' \exp(2\pi i fT')\langle [\![\mathbf{f}_c | \mathsf{L}\Delta\mathbf{u}(t, T) + \mathbf{S}(t, T)]\!]$$
$$\times [\![\mathbf{f}_c | \mathsf{L}\Delta\mathbf{u}(t, T + T') + \mathbf{S}(t, T + T')]\!]\rangle. \qquad (20)$$

In order for this formula to make sense, we must assume that T is sufficiently large that the autocorrelation function $\langle \Delta t'_c(T) \Delta t'_c(T + T') \rangle$ is stationary, *i.e.*, it is independent of T.

Example 3: In SESAM lasers, the modelocked pulse opens up a gain window in which noise grows in the wake of the pulse. This growth can lead to a wake instability [41, 67], but even when the wake is stable, it can lead to visible sidebands in the spectrum. In order to calculate the spectrum of the sidebands, we must determine the magnitude of the noise that enters the wake modes. We will see in Sec. 4 that there are two wake modes $\mathbf{e}_{w+} = [e_{w+}, \bar{e}_{w+}]^T$ and $\mathbf{e}_{w-} = [e_{w-}, \bar{e}_{w-}]^T$ with the property that $e_{w-} = \bar{e}^\star_{w+}$ and $\bar{e}_{w-} = e^\star_{w+}$. These modes are eigenmodes of the operator L that we defined in Eqs. (11) and (19). The contribution of the wake modes to the fluctuating power is given by $\Delta P_w = [\![\mathbf{u}_0 | \Delta \mathbf{u}_w]\!] = c_{w+}[\![\mathbf{u}_0 | \mathbf{e}_{w+}]\!] + c_{w-}[\![\mathbf{u}_0 | \mathbf{e}_{w-}]\!]$, where c_{w+} and c_{w-} are the amplitudes of the wake modes, which we define in Eqs. (23) and (24). We then find that the power spectral density is equal to

$$S_w(f) = \int\limits_{-\infty}^{\infty} dT' \exp(2\pi i f T')$$
$$\times \left\langle \left\{ [\![\mathbf{u}_0 | \Delta \mathbf{u}_w(T)]\!][\![\mathbf{u}_0 | \Delta \mathbf{u}_w(T + T')]\!] \right\} \right\rangle. \quad (21)$$

The advantage of expressing quantities of interest as inner products is that all these quantities can be found computationally for any $u_0(t)$ without solving the evolution equations once the spectrum of the operator L in Eq. (5) is known. Determining the spectrum is an eigenvalue problem for which powerful computational methods are available.

In developing the general formalism, we first recall from Eq. (19) that

$$\frac{\partial \Delta \mathbf{u}(t, T)}{\partial T} = \mathsf{L}\Delta \mathbf{u}(t, T) + \mathbf{S}(t, T'),$$

where $\bar{S}(t, T) = S^\star(t, T)$, and

$$\mathsf{L}(t) = \begin{bmatrix} L_{11}(t) & L_{12}(t) \\ L_{21}(t) & L_{22}(t) \end{bmatrix}, \quad (22)$$

where $L_{22} = L^\star_{11}$ and $L_{21} = L^\star_{12}$, so that if $\Delta \bar{u}(T = 0) = \Delta u^\star(T = 0)$, then Δu and $\Delta \bar{u}$ remain complex conjugates at all T. We now write $\Delta \mathbf{u}$ as a sum of eigenmodes of the operator L, so that

$$\Delta \mathbf{u} = \sum_{j=1}^{n} c_j \mathbf{e}_j + \frac{1}{2\pi} \int c(\varpi) \mathbf{e}(\varpi) \, d\varpi, \quad (23)$$

where $c_j = c_j(T)$ and $\mathbf{e}_j = \mathbf{e}_j(t)$, and we are assuming that there are n modes in the discrete spectrum, and we

are using a parameter ϖ to parameterize the continuous spectrum, which may have several branches. We are also assuming that L can be decomposed into a complete set of eigenmodes, *i.e.*, it is not defective. That is not necessarily the case; the operator for the linearized nonlinear Schrödinger equation is defective [65]. However, this situation is not usual in laser applications in which gain and loss is always present. If the decomposition in Eq. (23) is complete, then there is a complementary set of adjoint eigenvectors $\hat{\mathbf{e}}_j$ and $\hat{\mathbf{e}}(\varpi)$ that have the property [64]

$$[\![\hat{\mathbf{e}}_j | \Delta \mathbf{u}]\!] = c_j, \qquad [\![\hat{\mathbf{e}}(\varpi) | \Delta \mathbf{u}]\!] = c(\varpi). \quad (24)$$

From Eqs. (19) and (22), we infer the general results: (1) If λ_j is an eigenvalue of L with the eigenvector $[e_j, \bar{e}_j]^T$, then $\lambda^\star_j$ is also an eigenvalue with eigenvector $[\bar{e}^\star_j, e^\star_j]^T$. (2) If λ_j is real, the $\bar{e}_j = e^\star_j$. Corresponding results also hold for the continuous modes.

In computational studies, we necessarily restrict the time domain to a finite time window and consider a finite number of time points in that window. In these studies, the distinction between continuous and discrete modes disappears, although in the limit as the time window becomes infinite, all but a small number of eigenvalues coalesce into the continuous spectrum. Unfortunately, as we have discussed elsewhere [62], the convergence towards the continuous spectrum is poor, and a different approach is needed to find the continuous eigenvalues. We will not consider this issue further here, since it does not play a role in our subsequent discussion. We will be focusing here on the impact of the noise on the discrete modes. Hence, we will write $\Delta \mathbf{u} = \sum_{j=1}^{n} c_j \mathbf{e}_j$.

We consider first the timing jitter. We recall from Eq. (17) that $\langle t^2_c(T) \rangle = \langle [\![\mathbf{f}_c | \Delta \mathbf{u}]\!]^2 \rangle$, where $\mathbf{f}_c = t\mathbf{u}_0 / w_0$, and $\mathbf{u}_0 = [u_0, u^\star_0]^T$. We now find

$$\langle t^2_c(T) \rangle = \sum_{j=1}^{n} \sum_{k=1}^{n} \langle c_j(T) c_k(T) \rangle [\![\mathbf{f}_c | \mathbf{e}_j]\!][\![\mathbf{f}_c | \mathbf{e}_k]\!]. \quad (25)$$

In general, the $\mathbf{e}_j$ are not mutually orthogonal, and the correlation between the different modes cannot be neglected. In particular, we note that if $\lambda_k = \lambda^\star_j$, where λ_j has a nonzero imaginary part, then we must have $c_k(T) = c^\star_j(T)$ in order for Δu and $\Delta \bar{u}$ to remain complex conjugates if they are initially. So, these two amplitudes are perfectly correlated. We stress this point because it is a peculiarity of soliton perturbation theory that there are four degenerate discrete modes, all associated with eigenvalue zero, that can be chosen to be mutually orthogonal [65]. The presence of gain and loss breaks this degeneracy, and it is no longer possible to choose a mutually orthogonal set of modes. We return to this point when we review the Haus-Mecozzi theory [45].

We now calculate the evolution of the c_j. Substitution of Eq. (23) into Eq. (19) yields

$$\frac{dc_j}{dT} = \lambda_j c_j + [\![\hat{\mathbf{e}}_j | \mathbf{S}]\!], \qquad (26)$$

which is a Langevin process. Integrating this equation from $T = 0$, we find

$$c_j(T) = \int_0^T dT' \exp\left[\lambda_j(T - T')\right] [\![\hat{\mathbf{e}}_j | \mathbf{S}]\!], \qquad (27)$$

where we assume $c_j(0) = 0$. Then, we find

$$\left\langle c_j(T) c_k(T) \right\rangle = \int_0^T dT' \int_0^T dT'' \left\langle [\![\hat{\mathbf{e}}_j | \mathbf{S}]\!] [\![\hat{\mathbf{e}}_k | \mathbf{S}]\!] \right\rangle$$
$$\exp\left[\lambda_j(T - T') + \lambda_k(T - T'')\right]. \qquad (28)$$

Using now Eq. (5), we find

$$\left\langle c_j(T) c_k(T) \right\rangle = D_{jk} \int_0^T dT' \exp\left[(\lambda_j + \lambda_k)(T - T')\right]$$
$$= -\frac{D_{jk}}{\lambda_j + \lambda_k} \left\{ 1 - \exp\left[(\lambda_j + \lambda_k)T\right] \right\}, \qquad (29)$$

where

$$D_{jk} = D \int_{-\infty}^{\infty} dt \left[\hat{e}_j^{\star}(t)\hat{e}_k^{\star}(t) + \hat{e}_j^{\star}(t)\hat{e}_k^{\star}(t) \right]. \qquad (30)$$

We must have $\text{Re}(\lambda_j \leq 0)$ and $\text{Re}(\lambda_k \leq 0)$ for stability. If either $\text{Re}(\lambda_j)$ or $\text{Re}(\lambda_k)$ is non-zero, then the exponential contribution to Eq. (29) decays as $T \to \infty$, and the correlation reaches a steady state, which is needed to calculated the power spectral densities. In this case, we find that Eq. (29) becomes

$$\left\langle c_j(T) c_k(T) \right\rangle = -\frac{D_{jk}}{\lambda_j + \lambda_k}. \qquad (31)$$

If λ_j and λ_k are purely imaginary, then the correlation oscillates unless $\lambda_j = -\lambda_k$, as when $\lambda_j = \lambda_k = 0$, in which case

$$\left\langle c_j(T) c_k(T) \right\rangle = D_{jk} T, \qquad (32)$$

which corresponds to a random walk. Substitution of Eq. (29) into the expression $\left\langle t_c^2 \right\rangle = \left\langle [\![\mathbf{f}_c | \Delta \mathbf{u}]\!]^2 \right\rangle$ yields an explicit expression for the timing jitter, which we find in the next section.

We now turn to the calculation of the power spectral densities. Following Eq. (20), and after some calculation, we have

$$S_{f\text{rep}}(f) = \sum_j \sum_k \frac{\lambda_j \lambda_k P_{cj} P_{ck} D_{jk}}{(2\pi f + i\lambda_j)(2\pi f - i\lambda_k)}$$
$$- \sum_j \frac{2\lambda_j^2 P_{cj} D_{cj}}{(2\pi f)^2 - \lambda_j^2} + D_c, \qquad (33)$$

where $P_{cj} = [\![\mathbf{f}_c | \mathbf{e}_j]\!]$, $D_{cj} = D[\![\hat{\mathbf{e}}_j | \mathbf{f}_c]\!]$, and $D_c = 2D \int_{-\infty}^{\infty} |f_c(t)|^2 dt$.

We conclude by calculating an expression for the power spectral density of the wake modes. From Eq. (21), we can obtain after some calculation

$$S_{\text{w}}(f) = \frac{2D_1 P_{u\text{w}}^2}{(2\pi f)^2 + \lambda_{\text{w}}^2} + \frac{2D_1^{\star} P_{u\text{w}}^{\star 2}}{(2\pi f)^2 + \lambda_{\text{w}}^{\star 2}}$$
$$+ \frac{2D_2 |P_{u\text{w}}|^2}{\lambda_{\text{w}} + \lambda_{\text{w}}^{\star}} \left[\frac{\lambda_{\text{w}}}{(2\pi f)^2 + \lambda_{\text{w}}^2} + \frac{\lambda_{\text{w}}^{\star}}{(2\pi f)^2 + \lambda_{\text{w}}^{\star 2}} \right], \qquad (34)$$

where

$$P_{u\text{w}} = [\![\mathbf{u}_0 | \mathbf{e}_{\text{w}+}]\!],$$

$$D_1 = D \int_{-\infty}^{\infty} \hat{e}_{\text{w}+}^{\star}(t)\hat{e}_{\text{w}+}^{\star}(t) dt, \qquad (35)$$

$$D_2 = D \int_{-\infty}^{\infty} \left[\hat{e}_{\text{w}+}^{\star}(t)\hat{e}_{\text{w}+}(t) + \hat{e}_{\text{w}+}(t)\hat{e}_{\text{w}+}^{\star}(t) \right] dt.$$

3 Application to the HME With Fast Saturable Absorbers

The formalism that we have developed is very general. It can be applied to any equilibrium solution of any averaged laser equation. In this section, we show how this general formalism can be applied to the particular equation that Haus and Mecozzi [45] analyzed in the particular limit in which soliton perturbation theory holds. The differences with soliton perturbation theory are discussed. Finally, we show how this formalism can be used to reproduce the expression for the power spectral density that was given by Paschotta [43].

Haus and Mecozzi begin with the HME,

$$\frac{\partial u}{\partial T} = \left[-i\phi + v\frac{\partial}{\partial t} + \frac{g(|u|)}{2}\mathcal{D}_t - \frac{l}{2} - \frac{i\beta''}{2}\frac{\partial^2}{\partial t^2} \right.$$
$$\left. + i\gamma|u|^2 + \delta|u|^2 \right] u + S(t, T), \qquad (36)$$

where we are using the same notation as in Eq. (1), and $g(|u|)$ is given by Eq. (2). The zero-order equation that Haus and Mecozzi use is the nonlinear Schrödinger equation (NLSE),

$$\frac{\partial u_0}{\partial T} = -i\phi u_0 + v\frac{\partial u_0}{\partial t} + \frac{i}{2}|\beta''|\frac{\partial^2 u_0}{\partial t^2} + i\gamma|u_0|^2 u_0, \qquad (37)$$

where it is assumed that $\beta'' < 0$, as is required for the NLSE to have pulsed solutions. It will simplify our exposition to set $\gamma = 1$ and $|\beta''| = 1$. We can return to physical units by making the substitutions $t \to t/|\beta''|^{1/2}$, $u \to \gamma^{1/2}u$.

The most general stationary pulse solution to Eq. (37) is [36, 45, 65]

$$u_0 = A_0 \text{sech}\left[A_0(t - t_0)\right] \exp\left[-i\omega_0(t - t_0) + i\theta_0\right],$$

$$\phi = \frac{1}{2}\left(\omega_0^2 + A_0^2\right), \tag{38}$$

$$v = -\omega_0,$$

where A_0, t_0, ω_0, and θ_0 are four arbitrary parameters that correspond respectively to the pulse's amplitude, its central time ($t_0 = t_c$), its central frequency, and central phase. We find that the pulse energy $w_0 = \int_{-\infty}^{\infty} |u_0|^2 \, dt = 2A_0$. If we return to physical units, we find that Eq. (38) becomes

$$u_0 = A_0 \text{sech}\left[\left(\gamma/|\beta''|\right)^{1/2} A_0(t - t_0)\right]$$

$$\times \exp\left[-i\omega_0(t - t_0) + i\theta_0\right],$$

$$\phi = \frac{1}{2}\left(|\beta''| \omega_0^2 + \gamma A_0^2\right), \tag{39}$$

$$v = -|\beta''| \omega_0.$$

In order to make our discussion more compact, we will use the abbreviations

$$\begin{aligned} \mathcal{S} &= \text{sech}\left[A_0(t - t_0)\right], \\ \mathcal{T} &= \tanh\left[A_0(t - t_0)\right], \\ \mathcal{E} &= \exp\left[-i\omega_0(t - t_0) + i\theta_0\right], \\ \tau &= t - t_0, \end{aligned} \tag{40}$$

so that $u_0 = A_0\mathcal{S}\mathcal{E}$. Haus and Mecozzi did not include a non-zero ϕ and v in their equation. As a consequence, both the central time and central phase change linearly with T. However, in reviewing their work and comparing it to ours, it is useful to have a zero-order solution that is strictly stationary and so does not depend on T.

Without the noise contributions, Eq. (36) becomes

$$\frac{\partial u}{\partial T} = \left[-\frac{i}{2}\left(\omega_0^2 + A_0^2\right) - \omega_0\frac{\partial}{\partial t} + \frac{i}{2}\frac{\partial^2}{\partial t^2} + i|u|^2\right]u$$

$$+ \left[\frac{g - l}{2} + i\frac{g\omega_{\text{off}}}{2\omega_g}\frac{\partial}{\partial t} + \frac{g}{4\omega_g^2}\frac{\partial^2}{\partial t^2} + \delta|u|^2\right]u. \tag{41}$$

In general, this equation will have chirped hyperbolic-secant solutions — in other words, the chirp-free NLSE soliton in Eq. (38) is not an equilibrium solution of this equation — as was first pointed out in the context of lasers by Martinez et al. [30]. However, in order to apply soliton perturbation theory, the equilibrium solution must be chirp-free. For that reason, Haus and Mecozzi specialize their equation, setting

$$\delta = \frac{g(|u_0|)}{2\omega_g^2},$$

$$\omega_{\text{off}} = \omega_0/\omega_g, \tag{42}$$

$$g(|u_0|) - l = -\frac{g(|u_0|)}{2\omega_g^2}(\omega_0^2 + A_0^2).$$

In this case, Eq. (41) becomes

$$\frac{\partial u}{\partial T} = (1 - i\Gamma_0)\left[-\frac{i}{2}(\omega_0^2 + A_0^2) - \omega_0\frac{\partial}{\partial t} + \frac{i}{2}\frac{\partial^2}{\partial t^2} + i|u|^2\right]u$$

$$+ \Delta\Gamma\left[\omega_g^2 + i\omega_0\frac{\partial}{\partial t} + \frac{1}{2}\frac{\partial^2}{\partial t^2}\right]u, \tag{43}$$

where $\Gamma_0 = g(|u_0|)/2\omega_g^2$ and $\Delta\Gamma = \left[g(|u|) - g(|u_0|)\right]/2\omega_g^2$. The analysis of Haus and Mecozzi only strictly applies to this highly specialized equation, but it has been found that many of the qualitative features persist in more general situations [29, 44].

We now determine modes that correspond to the discrete spectrum of the linearized NLSE. If we make a small change in the soliton, we may write

$$\Delta u = f_A \Delta A + f_\theta \Delta\theta + f_\omega \Delta\omega + (f_t + \omega_0 f_\theta)\Delta t + \Delta u_c, \tag{44}$$

where Δu_c denotes the portion of the perturbation that goes into the continuum, rather than changing the soliton's parameters, and

$$\begin{aligned} f_A &= \mathcal{S}\mathcal{E} - \tau A_0\mathcal{S}\mathcal{T}\mathcal{E}, \\ f_\theta &= iA_0\mathcal{S}\mathcal{E}, \\ f_\omega &= -i\tau A_0\mathcal{S}\mathcal{E}, \\ f_t &= A_0^2\mathcal{S}\mathcal{T}\mathcal{E}. \end{aligned} \tag{45}$$

The extra term $\omega_0 f_\theta$ that is proportional to Δt in Eq. (44) removes the time shift due to the group velocity dispersion. We may write the linearized NLSE as

$$\frac{\partial \Delta\mathbf{u}}{\partial t} = \mathsf{L}_0 \Delta\mathbf{u}, \tag{46}$$

where, using the same definitions as in Eqs. (19) and (22),

$$L_{0,11}(t) = -\frac{i}{2}\left(\omega_0^2 + A_0^2\right) - \omega_0\frac{\partial}{\partial t} + \frac{i}{2}\frac{\partial^2}{\partial t^2} + 2iA_0^2\mathcal{S}^2,$$

$$L_{0,12}(t) = iA_0^2\mathcal{S}^2\mathcal{E}^2, \tag{47}$$

and $L_{0,21}(t) = L_{0,12}^\star(t)$, $L_{0,22}(t) = L_{0,11}^\star(t)$. Defining now $\mathbf{f}_j = [f_j, f_j^\star]^T$, where $j = A, \theta, \omega, t$, we find that $\mathbf{f}_\theta$ and $\mathbf{f}_t$ are eigenmodes of L_0 with eigenvalue zero. By contrast, we find $\mathsf{L}_0\mathbf{f}_A = A_0\mathbf{f}_\theta$ and $\mathsf{L}_0\mathbf{f}_\omega = -\mathbf{f}_t$, so that $\mathbf{f}_A$ and $\mathbf{f}_\omega$ are not eigenvectors of L_0, although they are eigenvectors of L_0^2. In the language of spectral theory, the operator L_0 is defective, and the eigenvalue 0 has algebraic multiplicity 4 and geometric multiplicity 2 [64]. While not eigenmodes, the vectors $\mathbf{f}_A$ and $\mathbf{f}_\omega$ are part of a complete decomposition of the operator L_0 that includes the four $\mathbf{f}_j$ and the continuous spectrum [65].

We can verify directly that the $\mathbf{f}_j$ are mutually orthogonal; however, they will not be orthogonal to the continuum. To obtain operators that are orthogonal to the continuum, we must find the modes of the adjoint operator $\mathsf{L}_0^\dagger$,

whose elements are given by $L_{0,11}^\dagger = -L_{0,11}$, $L_{0,12}^\dagger = L_{0,12}$, $L_{0,21}^\dagger = L_{0,21}$, and $L_{0,22}^\dagger = -L_{0,22}$. From these relations, we infer that

$$\mathsf{L}_0 \begin{bmatrix} f \\ \bar{f} \end{bmatrix} = \begin{bmatrix} h \\ \bar{h} \end{bmatrix} \quad \text{implies} \quad \mathsf{L}_0^\dagger \begin{bmatrix} if \\ -i\bar{f} \end{bmatrix} = \begin{bmatrix} -ih \\ i\bar{h} \end{bmatrix}. \tag{48}$$

It follows immediately that $\hat{\mathbf{f}}_A = C_A[if_\theta, -if_\theta^\star]^T$ and $\hat{\mathbf{f}}_\omega = C_\omega[if_t, -if_t^\star]^T$ are eigenvectors of $\mathsf{L}_0^\dagger$, while $\hat{\mathbf{f}}_\theta = C_\theta[if_A, -if_A^\star]^T$ and $\hat{\mathbf{f}}_t = C_t[if_\omega, -if_\omega^\star]^T$ are eigenvectors of $\mathsf{L}_0^{\dagger 2}$, where the C_j are any real constants. We now infer from general spectral theory that $[\![\hat{\mathbf{f}}_j | \Delta \mathbf{u}_c]\!] = 0$, as long as none of the modes that make up the continuum has a zero eigenvalue, which is the case. Haus and Islam [57] infer the same result from a physical argument. If we use

$$\begin{aligned}
\hat{f}_A &= \frac{1}{2}A_0 \mathcal{S}\mathcal{E}, \\
\hat{f}_\theta &= \frac{i}{2}(\mathcal{S} - A_0 \tau \mathcal{S}\mathcal{T})\mathcal{E}, \\
\hat{f}_\omega &= -\frac{i}{2}A_0 \mathcal{S}\mathcal{T}\mathcal{E}, \\
\hat{f}_t &= \frac{1}{2}\tau \mathcal{S}\mathcal{E},
\end{aligned} \tag{49}$$

then $[\![\hat{\mathbf{f}}_i | \mathbf{f}_j]\!] = \delta_{ij}$, where δ_{ij} is the Krönecker-delta function, and $i, j = A, \theta, \omega, t$. We also see that the $\hat{\mathbf{f}}_j$, like the $\mathbf{f}_j$, are mutually orthogonal. If we now substitute Eq. (44) into Eq. (43), we find

$$\begin{aligned}
\frac{\partial \Delta u}{\partial T} &= f_A \frac{\mathrm{d}\Delta A}{\mathrm{d}T} + f_\theta \frac{\mathrm{d}\Delta\theta}{\mathrm{d}T} + f_\omega \frac{\mathrm{d}\Delta\omega}{\mathrm{d}T} \\
&\quad + (f_t + \omega_0 f_\theta)\frac{\mathrm{d}\Delta t}{\mathrm{d}T} + \frac{\partial \Delta u_c}{\partial T} \\
&= (1 - i\Gamma_0)(-A_0^2 \mathcal{S}\mathcal{T}\mathcal{E}\Delta\omega + iA_0^2 \mathcal{S}\mathcal{E}\Delta A) \\
&\quad + \Gamma'\left[\frac{1}{2}(2\omega_g^2 + \omega_0^2 + A_0^2)A_0 \mathcal{S}\mathcal{E} - A_0^3 \mathcal{S}^3 \mathcal{E}\right]\Delta A \\
&\quad + \Delta r_c,
\end{aligned} \tag{50}$$

where $\Gamma' = \mathrm{d}\Delta\Gamma/\mathrm{d}A$, and Δr_c is the residual contribution from the continuous waves, and we have made use of Eqs. (37) and (38). Combining Eq. (50) with its complex conjugate equation to obtain $\Delta \mathbf{u}$ and operating on the resulting vector equation with $\hat{\mathbf{f}}_j$, $j = A, \theta, \omega, t$, we obtain the four equations

$$\begin{aligned}
\frac{\mathrm{d}\Delta A}{\mathrm{d}T} &= 2\left[\Gamma_0 A_0^2 - g_s\left(1 + \frac{\omega_0^2}{2\omega_g^2} - \frac{A_0^2}{6\omega_g^2}\right)\right]\Delta A \\
&\equiv -\alpha_A \Delta A, \\
\frac{\mathrm{d}\Delta\theta}{\mathrm{d}T} &= A_0 \Delta A + \omega_0 \Delta\omega, \\
\frac{\mathrm{d}\Delta\omega}{\mathrm{d}T} &= -\frac{2}{3}\Gamma_0 A_0^2 \Delta\omega \equiv -\alpha_\omega \Delta\omega, \\
\frac{\mathrm{d}\Delta t}{\mathrm{d}T} &= -\Delta\omega,
\end{aligned} \tag{51}$$

where

$$\begin{aligned}
g_s &= -\Gamma' A_0 \omega_g^2 \\
&= -\frac{A_0}{2}\left.\frac{\mathrm{d}g(|u_0|)}{\mathrm{d}A}\right|_{A=A_0} \\
&= -A_0 \left.\frac{\mathrm{d}g}{\mathrm{d}w}\right|_{w=w_0}.
\end{aligned} \tag{52}$$

Equation (51) was obtained by Haus and Mecozzi with the exception of the third term in the parenthesis multiplying g_s, which they missed. We see that small changes in the amplitude will lead to a phase rotation, while a small shift in the frequency will lead to drift in the central time.

We now determine the stability of the equilibrium solution given by Eq. (38). We first find that small changes in the frequency always decay. Hence, the frequency mode is always stable. By contrast, the amplitude mode will only be stable if

$$2g_s\left(1 + \frac{\omega_0^2}{2\omega_g^2} - \frac{A_0^2}{6\omega_g^2}\right) > 2\Gamma_0 A_0^2, \tag{53}$$

and we see that gain saturation plays a critical role in determining the stability of the amplitude mode. The stability criterion for continuous waves is $l > g(|u_0|)$. These two stability criteria define a stability range that is narrower than what is observed in experiments, but identify instability mechanisms that are valid for a broad range of problems [26].

We now focus on the noise contributions. We have $\partial \Delta u / \partial T|_N = S(t, T)$, where we use N to denote noise-driven quantities. The statistics for a change in Δu over a time ΔT is given by

$$\begin{aligned}
\langle \Delta u_N(t, T)\Delta u_N^\star(t', T')\rangle &= D\delta(t - t')\delta(T - T')(\Delta T)^2, \\
\langle \Delta u_N(t, T)\Delta u_N(t', T')\rangle &= \langle \Delta u_N^\star(t, T)\Delta u_N^\star(t', T')\rangle = 0.
\end{aligned} \tag{54}$$

Writing now, $\Delta u_N = f_A \Delta A_N + f_\theta \Delta\theta_N + f_\omega \Delta\omega_N + (f_t + \omega_0 f_\theta)\Delta t_N$, we find

$$\begin{aligned}
&\langle \Delta A_N(T)\Delta A_N(T')\rangle \\
&= 2\int_{-\infty}^{\infty}\mathrm{d}t\int_{-\infty}^{\infty}\mathrm{d}t'\,\hat{f}_A^\star(t)\hat{f}_A(t')\langle \Delta u_N(t, T)\Delta u_N(t', T')\rangle \\
&= DA_0\delta(T - T')(\Delta T)^2.
\end{aligned} \tag{55}$$

Defining

$$\begin{aligned}
\left.\frac{\mathrm{d}\Delta A}{\mathrm{d}T}\right|_N &= S_A(T), \\
\langle S_A(T)S_A(T')\rangle &= D_A\delta(T - T'),
\end{aligned} \tag{56}$$

we conclude $D_A = DA_0$. In a similar way, we can show

$$\left.\frac{\mathrm{d}\Delta\theta}{\mathrm{d}T}\right|_N = S_\theta(T) - \omega_0 S_t(T),$$

$$\left.\frac{\mathrm{d}\Delta\omega}{\mathrm{d}T}\right|_N = S_\omega(T), \tag{57}$$

$$\left.\frac{\mathrm{d}\Delta t}{\mathrm{d}T}\right|_N = S_t(T),$$

where, letting $\langle S_j(T)S_j(T')\rangle = D_j\delta(T - T')$, we have

$$D_\theta = \frac{D}{3A_0}\left(1 + \frac{\pi^2}{12}\right),$$

$$D_\omega = \frac{DA_0}{3}, \tag{58}$$

$$D_t = \frac{D}{A_0^3}\frac{\pi^2}{12}.$$

We note that $D_t = D_c$, where D_c is defined after Eq. (33). These results were first derived by Haus and Mecozzi [45] with a correction that was found by Paschotta [43]. It is a consequence of the mutual orthogonality of the $\mathbf{f}_j$ that the S_j are uncorrelated for $j \neq k$. While the noise driver for $\Delta\theta$ is in general correlated with the noise driver for Δt, it is possible to avoid this difficulty by specializing to the case $\omega_0 = 0$, which is what Haus and Mecozzi do. There is no real loss of generality, since one is always free to pick the carrier frequency for convenience.

Making this choice, we find that Eq. (51) becomes

$$\frac{\mathrm{d}\Delta A}{\mathrm{d}T} = -\alpha_A\Delta A + S_A, \tag{59a}$$

$$\frac{\mathrm{d}\Delta\theta}{\mathrm{d}T} = A_0\Delta A + S_\theta, \tag{59b}$$

$$\frac{\mathrm{d}\Delta\omega}{\mathrm{d}T} = -\alpha_\omega\Delta\omega + S_\omega, \tag{59c}$$

$$\frac{\mathrm{d}\Delta t}{\mathrm{d}T} = -\Delta\omega + S_t. \tag{59d}$$
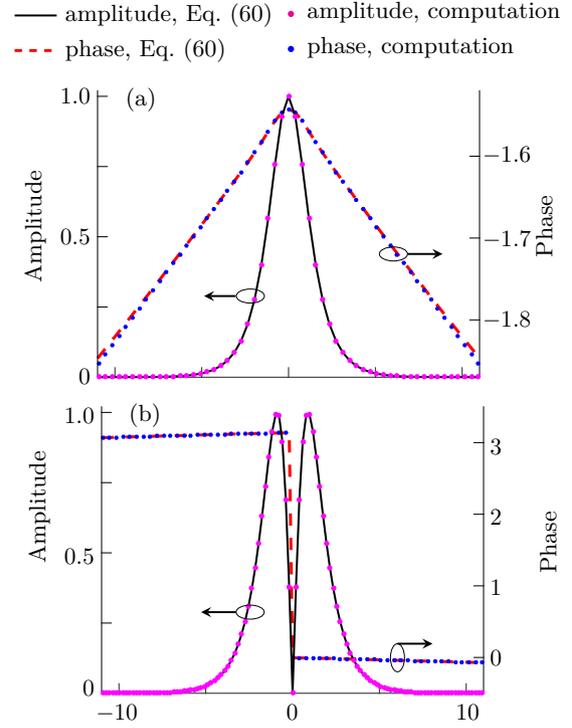
The pair of equations (59a) and (59b) and the pair of equations (59c) and (59d) are both examples of a Gordon process [68, 69]. In the case of timing jitter, the stochastic differential equations (59c) and (59d) may be integrated to yield

$$\langle(\Delta t)^2\rangle = \left(D_t + \frac{1}{\alpha_\omega^2}D_\omega\right)T - \frac{2D_\omega}{\alpha_\omega^3}\left[1 - \exp(-\alpha_\omega T)\right]$$

$$+ \frac{D_\omega}{2\alpha_\omega^3}\left[1 - \exp(-2\alpha_\omega T)\right]. \tag{60}$$

A similar expression can be obtained for $\langle(\Delta\theta)^2\rangle$.

In order to apply the general formalism to this problem, we must first identify the modes of L and $\mathsf{L}^\dagger$. From Eqs. (50) and (51), setting $\omega_0 = 0$ and neglecting the continuum, we have

$$\frac{\partial\Delta u}{\partial T} = f_A\frac{\mathrm{d}\Delta A}{\mathrm{d}T} + f_\theta\frac{\mathrm{d}\Delta\theta}{\mathrm{d}T} + f_\omega\frac{\mathrm{d}\Delta\omega}{\mathrm{d}T} + f_t\frac{\mathrm{d}\Delta t}{\mathrm{d}T}$$

$$= A_0 f_\theta\Delta A - f_t\Delta\omega - \alpha_A f_A\Delta A - \alpha_\omega f_\omega\Delta\omega. \tag{61}$$

Figure 1: The eigenmodes due to (a) the amplitude and (b) the central frequency perturbation.

We infer

$$\mathsf{L}\mathbf{f}_A = A_0\mathbf{f}_\theta - \alpha_A\mathbf{f}_A,$$

$$\mathsf{L}\mathbf{f}_\theta = 0,$$

$$\mathsf{L}\mathbf{f}_\omega = -\mathbf{f}_t - \alpha_\omega\mathbf{f}_\omega, \tag{62}$$

$$\mathsf{L}\mathbf{f}_t = 0,$$

so that the eigenfunctions of the operator L are

$$\mathbf{e}_A = \mathbf{f}_A - \frac{A_0}{\alpha_A}\mathbf{f}_\theta,$$

$$\mathbf{e}_\theta = \mathbf{f}_\theta,$$

$$\mathbf{e}_\omega = \mathbf{f}_\omega + \frac{1}{\alpha_\omega}\mathbf{f}_t, \tag{63}$$

$$\mathbf{e}_t = \mathbf{f}_t,$$

with respectively the eigenvalues $-\alpha_A$, 0, $-\alpha_\omega$, 0.

It cannot be too strongly stressed that $\mathbf{f}_A$ and $\mathbf{f}_\omega$ are not eigenmodes of the operator L and that the actual eigenmodes are not mutually orthogonal. As a result, the amplitudes of the eigenmodes will be correlated. This issue was a source of confusion in a recent experiment that found the eigenmodes of a modelocked laser [70].

In Fig. 1, we show a comparison between the amplitude and frequency modes of the HME that our algorithm finds [62] and are predicted by Eq. (63). The parameter set is $g_0 = 0.2$, $l = 0.11$, $\omega_g = \sqrt{5}$, $\omega_0 = 0$, $P_{\mathrm{sat}}T_R = 2$, and $\delta = 0.01$. For both the amplitude and the phase of the

eigenmodes, the agreement between our computational results and the perturbation theory [Eq. (63)] is excellent. The eigenvalues that the perturbation theory predicts are $\alpha_\omega = 0.0283$ and $\alpha_A = 0.00667$, while our algorithm obtained the same result.

We can construct the adjoint eigenvectors that are biorthogonal to the $\mathbf{e}_j$ from the $\hat{\mathbf{f}}_j$. They are

$$
\begin{aligned}
\hat{\mathbf{e}}_A &= \hat{\mathbf{f}}_A, \\
\hat{\mathbf{e}}_\theta &= \hat{\mathbf{f}}_\theta + \frac{A_0}{\alpha_A}\hat{\mathbf{f}}_A, \\
\hat{\mathbf{e}}_\omega &= \hat{\mathbf{f}}_\omega, \\
\hat{\mathbf{e}}_t &= \hat{\mathbf{f}}_t - \frac{1}{\alpha_\omega}\hat{\mathbf{f}}_\omega.
\end{aligned}
\tag{64}
$$

Noting that the timing jitter function that appears in Eq. (17) may be written as $\mathbf{f}_c(t) = \hat{\mathbf{f}}_t(t) = \hat{\mathbf{e}}_t(t) + (1/\alpha_\omega)\hat{\mathbf{e}}_\omega(t)$, we find

$$
\begin{aligned}
\langle (\Delta t)^2 \rangle &= \left\langle \left(c_t + \frac{1}{\alpha_\omega}c_\omega \right)^2 \right\rangle \\
&= \frac{1}{\alpha_\omega^2}\langle c_\omega^2 \rangle + \frac{2}{\alpha_\omega}\langle c_\omega c_t \rangle + \langle c_t^2 \rangle.
\end{aligned}
\tag{65}
$$

Using now Eq. (29), we have

$$
\begin{aligned}
\langle c_\omega^2 \rangle &= \frac{1}{2\alpha_\omega}\left[1 - \exp(-2\alpha_\omega T) \right] \int_{-\infty}^{\infty} 2D|\hat{\mathbf{e}}_\omega|^2 \, dt \\
&= \frac{D_\omega}{2\alpha_\omega}\left[1 - \exp(-2\alpha_\omega T) \right]
\end{aligned}
\tag{66}
$$

and similarly

$$
\begin{aligned}
\langle c_\omega c_t \rangle &= -\frac{D_\omega}{\alpha_\omega^2}\left[1 - \exp(-\alpha_\omega T) \right], \\
\langle c_t^2 \rangle &= \left(D_t^2 + \frac{1}{\alpha_\omega^2}D_\omega \right) T.
\end{aligned}
\tag{67}
$$

Substitution of Eqs. (66) and (67) into Eq. (65) yields Eq. (60) once again. The derivation of this result is in fact somewhat simpler than the direct calculation of Eq. (60) since we have effectively decomposed the Gordon process into two Langevin processes and a random walk.

We finally turn to the calculation of the power spectral density. After substitution into Eq. (33), we find

$$
S_{f\text{rep}} = \frac{D_\omega}{(2\pi f)^2 + \alpha_\omega^2} + D_t,
\tag{68}
$$

where we note that $\lambda_\omega = -\alpha_\omega$, $\sum_j \sum_k P_{cj}P_{ck} = D_\omega/\alpha_\omega^2$, and $\lambda_j D_{cj} = 0$ for all j. Our result matches Paschotta's [43].

4 Application to the HME With a Slow Saturable Absorber

We now turn to consideration of modelocking with a slow saturable absorber. We note that by "slow," we mean that the absorber response time is long compared to the pulse duration, but — unlike the saturable gain — is short compared to the round-trip time. In addition to the possibility of continuous waves becoming unstable and the amplitude mode becoming unstable, it is possible for wake modes — modes that grow in the wake of the soliton — to become unstable. Even when stable, these modes can produce observable sidebands on the teeth of a locked comb.

The stability of these wake modes was analyzed by Kärtner et al. [41]. It is difficult to use soliton perturbation theory for this purpose. It is a basic assumption of the theory that the spectrum of the linearized equation has the same structure as the spectrum of the linearized NLSE, which has a continuous spectrum and four discrete modes. That is the case for the HME with a fast saturable absorber, although we have seen that the actual amplitude and frequency eigenmodes are different in practice from the amplitude and frequency modes that Haus [29] used. However, it is not the case for the HME with a slow saturable absorber. For typical parameters, there are six discrete eigenmodes — including two modes with complex conjugate eigenvalues that correspond to the wake. We show a typical spectrum in a case where the system is stable in Fig. 2. The system parameters are $g_0 = 0.25$, $l = 0.09$, $\omega_g = \sqrt{10}$, $\omega_0 = 0$, $P_{\text{sat}}T_R = 2$, $\tau_A = 18$, $w_A = 1$, and $\rho = 0.005$. As shown in Fig. 2(a), the spectrum includes the soliton spectrum elements — the two branches of the continuous spectrum and four discrete eigenvalues on the real axis — and also two extra discrete eigenvalues that are complex conjugates and that correspond to the wake modes. When the small-signal gain increases or the dispersion decreases, the eigenvalues corresponding to the wake modes move to the right of the imaginary axis, and the modelocked pulse becomes unstable *via* a Hopf bifurcation, as shown with the arrows in Fig. 2(b).

Analyzing this system is no problem for our general formalism, which can in principle deal with any pulse shape and with any number of discrete modes. As we have shown, this formalism can even deal with edge bifurcations, in which new discrete eigenmodes bifurcate out of the continuum [62]. By contrast, analyzing this system with soliton perturbation theory is difficult and requires a substantial modification of the theory. At the same time, it does provide some analytical insights. In this section, we review the work of Kärtner et al. [41], contrasting their
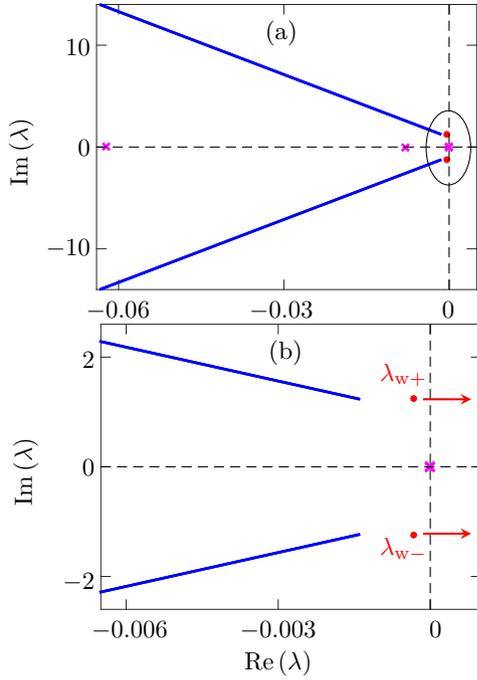
Figure 2: The spectrum of a modelocked laser model with a slow saturable absorber, where in (b), we show the spectrum near the origin of (a). From left to right in (a) on the real axis, the discrete modes are the amplitude mode, the frequency mode, and the phase and time modes. The last two modes have eigenvalue zero.

approach to our general formalism, and we compare our prediction to theirs for when the wake modes become unstable. Finally, we calculate the power spectral density of the sidebands.

In this section, like in the last section, we will set $|\beta''| = 1$, $\gamma = 1$, and $\omega_0 = 0$. We will also set $t_0 = 0$ and $\theta_0 = 0$. These choices can be made with no real loss of generality.

The starting point of Kärtner et al. [41] is the observation by Gordon [71] that there is a function that evolves linearly and that is associated with the continuous waves of the NLSE. Explicitly, we find that if we solve the following linear equation for v, given a continuum wave Δu_c,

$$\Delta u_c(t, T) = -\frac{\partial^2 v(t, T)}{\partial t^2} + 2A_0 \mathcal{T} \frac{\partial v(t, T)}{\partial t} - A_0^2 \mathcal{T}^2 v(t, T) + A_0^2 \mathcal{S}^2 \mathcal{E}^2 v^\star(t, T), \qquad (69)$$

then $v(t, T)$ obeys the dispersive wave equation

$$\frac{\partial v(t, T)}{\partial T} = -\frac{iA_0^2}{2} v(t, T) + \frac{i}{2} \frac{\partial^2 v(t, T)}{\partial t^2}, \qquad (70)$$

where we recall that with our choice for t_0 and θ_0, $\mathcal{T} = \tanh(A_0 t)$, $\mathcal{S} = \mathrm{sech}(A_0 t)$, and $\mathcal{E} = 1$. If we perturb the equation for Δu by adding gain and loss, then we will perturb the equation for v, but the equation for v does not contain the Kerr nonlinearity [71]. This perturbed equation will

itself have a discrete and a continuous spectrum. The discrete spectrum corresponds to the wake modes, and when the wake modes in the spectrum of the equation for v become unstable, then the corresponding wake modes in the equation for Δu become unstable. This somewhat roundabout procedure, where we first divide the perturbed spectrum into four discrete modes and a continuum and then divide that continuum into two discrete modes and a different continuum is not conceptually simple or generalizable, but it does yield an analytical prediction for when instability will occur in this particular case.

Now we apply our method. The first step is to obtain an equation for v from the equation for Δu. We have set $\omega_{\text{off}} = 0$ in Eq. (11) to be consistent with setting $\omega_0 = 0$, and we find

$$\begin{aligned}
\frac{\partial \Delta u}{\partial T} &= \left(-\frac{iA_0^2}{2} + i\frac{\partial^2}{\partial t^2} + 2i|u_0|^2 \right) \Delta u + iu_0^2 \Delta \bar{u} \\
&+ \left[\frac{g(|u_0|)}{2} \left(1 + \frac{1}{2\omega_g^2} \frac{\partial^2}{\partial t^2} \right) - \frac{l}{2} - \rho n(|u_0|) \right. \\
&\left. -\rho u_0 \frac{\mathrm{D}n}{\mathrm{D}u} \cdot \right] \Delta u - \rho u_0 \frac{\mathrm{D}n}{\mathrm{D}\bar{u}} \cdot \Delta \bar{u} \\
&+ \frac{1}{2} \left[\frac{\mathrm{D}g}{\mathrm{D}u} \cdot \Delta u + \frac{\mathrm{D}g}{\mathrm{D}\bar{u}} \cdot \Delta \bar{u} \right] \mathcal{D}_t u_0 \\
&= (L_{0,11} + L_{1,11})\Delta u + (L_{0,12} + L_{1,12})\Delta \bar{u}. \qquad (71)
\end{aligned}$$

The quantities $L_{0,11}$ and $L_{0,12}$ are the operators for the linearized NLSE that we defined in Eq. (47). Setting $\omega_0 = 0$, we obtain

$$\begin{aligned}
L_{1,11} &= \frac{g(|u_0|)}{2} \left(1 + \frac{1}{2\omega_g^2} \frac{\partial^2}{\partial t^2} \right) - \frac{l}{2} - \rho n - \rho u_0 \frac{\mathrm{D}n}{\mathrm{D}u}, \\
L_{1,12} &= -\rho u_0 \frac{\mathrm{D}n}{\mathrm{D}\bar{u}}. \qquad (72)
\end{aligned}$$

We note that $L_{1,12}$, like $L_{0,12}$, is proportional to u_0, so that Δu and $\Delta \bar{u}$ will be uncoupled away from the modelocked pulse. Kärtner et al. completely neglect this coupling, which seems reasonable for perturbations due to the wake modes since they exist largely at fast times for which $u_0 \simeq 0$. With this approximation, we obtain

$$\begin{aligned}
L_{1,11} &= \frac{g(|u_0|)}{2} \left(1 + \frac{1}{\omega_g^2} \frac{\partial^2}{\partial t^2} \right) - \frac{l}{2} - \rho n, \\
L_{1,12} &= 0. \qquad (73)
\end{aligned}$$

Writing

$$\frac{\partial \Delta \mathbf{u}}{\partial T} = (\mathsf{L}_0 + \mathsf{L}_1)\Delta \mathbf{u}, \qquad (74)$$

and $\mathsf{M}\mathbf{v} = \Delta \mathbf{u}$, where from Eq. (69), M is the 2×2 time-dependent operator whose elements are given by

$$\begin{aligned}
M_{11} &= -\frac{\partial^2}{\partial t^2} + 2A_0 \mathcal{T} \frac{\partial}{\partial t} - A_0^2 \mathcal{T}^2, \\
M_{12} &= A_0^2 \mathcal{S}^2 \mathcal{E}^2, \qquad (75)
\end{aligned}$$

with $M_{21} = M_{12}^\star$ and $M_{22} = M_{11}^\star$, we now find

$$\frac{\partial \mathbf{v}}{\partial T} = M^{-1}L_0\Delta\mathbf{u} + M^{-1}L_1\Delta\mathbf{u}$$
$$= D\mathbf{v} + L_1\mathbf{v} + (M^{-1}L_1 - L_1M^{-1})\Delta\mathbf{u}, \quad (76)$$

where D is the 2×2 time-dependent operator whose elements are given by $D_{11} = -iA_0^2/2 + i\partial^2/\partial t^2$, $D_{12} = D_{21} = 0$, $D_{22} = D_{11}^\star$, and M^{-1} is the Green's function that is the inverse of M. If M^{-1} and L_1 commute, then Eq. (76) becomes simply

$$\frac{\partial \mathbf{v}}{\partial T} = D\mathbf{v} + L_1\mathbf{v} \equiv L_K\mathbf{v}. \quad (77)$$

In fact, the operators L_1 and M^{-1} do not commute, but Kärtner et al. argue by analogy to work on actively mode-locked lasers that the additional contributions from the commutator are negligible [72]. Within these approximations, v is decoupled from $v^\star$, and we obtain a linear equation for v,

$$\frac{\partial v}{\partial T} = L_{K,11}v$$
$$= -\frac{iA_0^2}{2} + \frac{i}{2}\frac{\partial^2 v}{\partial t^2} + \frac{g(|u_0|)}{2}\left(1 + \frac{2}{\omega_g^2}\frac{\partial^2}{\partial t^2}\right)v$$
$$- \frac{l}{2}v - \rho n(|u_0|)v. \quad (78)$$

This equation is the usual linear Schrödinger equation, with the difference that $L_{K,11}$ is not anti-Hermitian, and the eigenvalues will have real as well as imaginary components. The sign of the real part of the discrete eigenvalue of the ground state λ_K determines the stability of the wake modes. Explicit expressions for the wake modes may in principle be obtained by solving Eq. (78) for the eigenmode $\mathbf{v}$ and then using Eq. (69) to obtain $\Delta u = \Delta u_c$. The corresponding wake modes are $\Delta\mathbf{u}_{w+} = [\Delta u, 0]^T$ and $\Delta\mathbf{u}_{w-} = [0, \Delta u^\star]^T$, with eigenvalues λ_K and $\lambda_K^\star$, respectively.

Kärtner et al. [41] considered two different approximations to $n(|u_0|)$ in order to obtain an analytical solution for this equation. In the simplest of these approximations, which is a V-shaped response, they set

$$n(|u_0|) = \begin{cases} \infty, & t < 0 \\ t/t_A, & t > 0 \end{cases} \quad (79)$$

where t_A is the response time of the SESAM. Setting $\partial v_K/\partial T = \lambda_K v_K$ in Eq. (78), we find the solution

$$v_K = C\text{Ai}\left[-r(t + t_{\text{off}})\right], \quad (80)$$

where C is an arbitrary constant, $\text{Ai}(\cdot)$ is the Airy function [73], $r = (\rho/t_A)^{1/3}(i + g/4\omega_g^2)^{-1/3} \simeq \exp(-i\pi/3)(\rho/t_A)^{1/3}$, and $t_{\text{off}} = (t_A/\rho)\left[\lambda_K - (1/2)(g - l) + iA_0^2/2\right]$. We note that $g/4\omega_g^2 \ll 1$
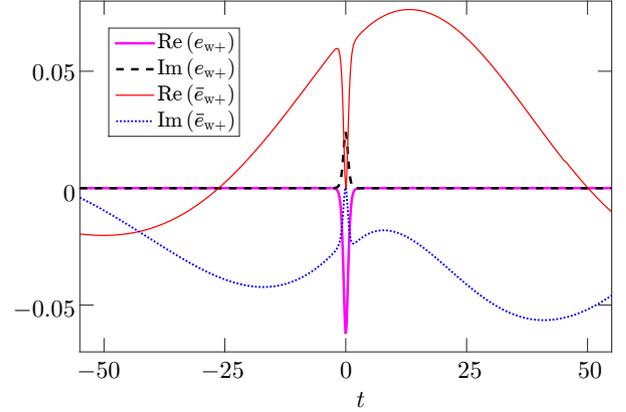

Figure 3: The profile of the wake mode near $t = 0$. The sharp spike in all curves around $t = 0$ corresponds to the location of the mode-locked pulse.

is required for the perturbation expansion to be valid. We have the boundary condition $v_K(0) = \text{Ai}(rt_{\text{off}}) = 0$, so that $rt_{\text{off}} = \exp(-i\pi/6)(\rho/t_A)^{-2/3}\left[\lambda_K - (1/2)(g - l) + iA_0^2/2\right] = -2.84$. The real part of λ_K is given by

$$\text{Re}(\lambda_K) = (1/2)(g - l) - 1.46(\rho/t_A)^{2/3}, \quad (81)$$

which is essentially the result of Kärtner et al. [41]. We note the additional offset of $-iA_0^2/2$ in the imaginary part of λ_K. This offset appears because we started with a stationary equilibrium solution and corresponds to the frequency difference between the modelocked pulse and the dispersive waves. This same offset is actually present in the theory of Kärtner et al., but it is carried by the modelocked pulse. That is inconvenient if one wishes to go beyond determining the stability of the wake modes and calculate their profile and their power spectral density in the presence of noise because in that case one must include both the wake mode with eigenvalue λ_{w+} and the wake mode with eigenvalue $\lambda_{w-} = \lambda_{w+}^\star$.
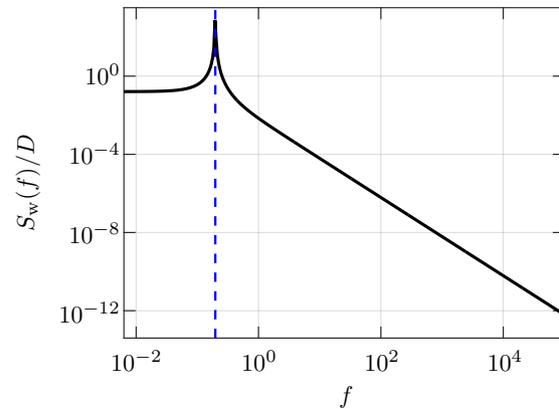
We can now compare the results of our general formula, given in Eq. (34) to the Kärtner et al. results. We use the same set of parameters as in Fig. 2, and we use the computational method that is described in [62] to calculate the wake mode $\mathbf{e}_{w+}$. In Fig. 3, we show the real and imaginary parts of both e_{w+} and $\bar{e}_{w+}$. We observe that $e_{w+} = 0$ away from the modelocked pulse, which is consistent with Eq. (72). By contrast both the real and imaginary parts of $\bar{e}_{w+}$ extend far beyond the gain window that is opened up by the slow saturable absorber, and we only show the central portion of their profile. In Fig. 4, by assuming $t_A = \tau_A$, we compare, as τ_A varies, the real parts of the eigenvalue of the wake mode that are derived using two different approaches. We obtained $\text{Re}(\lambda_{w+})$ computationally using Eq. (13), which is the analytical solution of
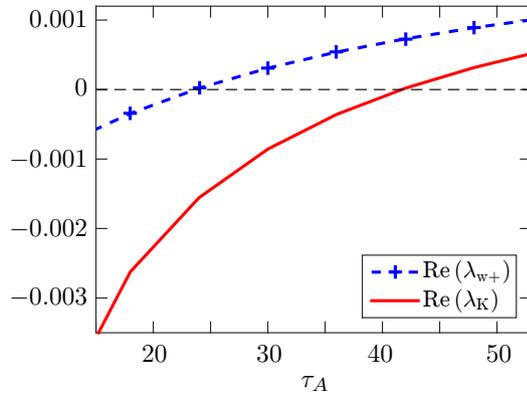
Figure 4: The variation of the real part of the eigenvalue corresponding to the wake modes, where $\mathrm{Re}\,(\lambda_{\mathrm{w+}})$ is derived using the computational method that is described in [62], and λ_{K} is calculated using Eq. (81).

Figure 5: An illustration of the power spectral density that is calculated using Eq. (34). The dashed line corresponds to the minimum frequency offset of the continuous spectrum which equals $A_0^2/(4\pi)$.

Eq. 4, while $\mathrm{Re}\,(\lambda_{\mathrm{K}})$ is calculated using Eq. (81), in which Eq. (79) is used to approximate Eq. (13). As the response time of the absorber decreases from $\tau_A = 54$ to $\tau_A = 15$, both $\mathrm{Re}\,(\lambda_{\mathrm{w+}})$ and $\mathrm{Re}\,(\lambda_{\mathrm{K}})$ decrease, which indicates that the modelocked system becomes more stable. We recall that wake modes become unstable due to the nonlinear growth of the modes in the gain window that opens up in the wake of the pulse [41, 67]. The duration of the gain window decreases as τ_A decreases, which in turn will help stabilize the modelocked pulse, which agrees qualitatively with the result in Fig. 4. Meanwhile, in the approximation of Eq. (79), the duration of the time window is smaller than the analytical response in Eq. (13) [41]. Hence we see that $\mathrm{Re}\,(\lambda_{\mathrm{K}}) < \mathrm{Re}\,(\lambda_{\mathrm{w+}})$ for all the cases that we consider. The modelocked system becomes unstable at $\tau_A \approx 23.7$ according to our calculation, while using Kärtner *et al.*'s approximation predicts the system becomes unstable when $\tau_A \approx 41$, which underestimates the destablizing effect of the wake modes.

Using Eq. (34), we show in Fig. 5 the calculated two-sided power spectral density $S_{\mathrm{w}}(f)$ using the same set of parameters as in Fig. 2. We recall that f is normalized by T_R^{-1} and the power is normalized with respect to γ, where γ is the nonlinear phase change per unit power per roundtrip. We find that there exists a peak near the minimum frequency offset of the continuous spectrum which equals $A_0^2/(4\pi)$. This peak corresponds to a modulation of the modelocked pulse, which will be visible in experiments as sidebands on the comb teeth of the power spectral density.

5 Discussion and Conclusions

We stated at the outset that our goal is to take full advantage of 150 years of mathematical developments in dynamical systems theory and spectral methods as well as 50 years of advances in computational methods to develop algorithms that can efficiently determine the stable operating regimes of passively modelocked lasers. We believe that the algorithms that we have developed fully meet this goal for averaged models, although considerable more work could be done to optimize these algorithms. We previously showed that we could map the stability boundaries in a two-dimensional parameter space, and we show here that we can calculate the impact of noise on both the timing jitter and the power spectral density without carrying out Monte Carlo simulations.

The model that we use in this article is an extension of the Haus modelocking equation. Additional components are usually included in more realistic and specialized models of modern-day passively modelocked laser systems. In some solid-state lasers, the gain recovery time is short enough to lead to relaxation oscillations. In this case, the partial differential equations that describe the evolution of the light envelope in the cavity must be supplemented by ordinary differential equations that describe the evolution of the gain [74]. Similarly, in order to further stabilize the laser against phase noise, modern day comb lasers include electronic feedback systems that remove the phase and time invariance, which once again lead to equations in which ordinary differential equations are coupled to the partial differential equations that describe the evolution of the light envelope [75]. In both cases, new degrees-of-freedom are introduced that lead to new discrete modes, but the basic algorithms do not have to be changed.

At this point, we can think seriously about how to extend this approach to full models. In this case, the equilibrium solution will not be stationary as it passes through the laser in one round trip; it will only be periodically stationary. If we represent the elements of the laser — the fibers, couplers, amplifiers, saturable absorbers, and so on — as operators on a pulse in the laser, then at any particular point in the laser, we write that

$$u(t, T + 1) = M_n M_{n-1} \cdots M_1 u(t, T) \equiv M u(t, T), \quad (82)$$

where $M_1, M_2, \ldots, M_1$ are the mathematical operators that represent the devices in the laser, and M represents the combined action of all these operators. In our case, we would search for a periodically-stationary solution that satisfies the relation

$$u_0(t, T + 1) = M u_0(t, T) = u_0(t, T). \quad (83)$$

In a regime where the pulse is highly stable, we can use an evolutionary code to find a stable solution. From there, we can vary the model parameters slowly and solve a root-finding problem that is the same as the root-finding problem in the averaged models, with the important difference that every iteration requires an integration over one round trip of the laser. Nijhof et al. [76] for example have discussed how to efficiently carry out this task. When an equilibrium is found, we can investigate the stability of the system by perturbing the system using a complete set of modes, integrating over one round trip, and creating a transformation matrix. Holzlöhner et al. [77] and Deconninck and Kutz [78] have discussed algorithms for carrying out this task. The eigenmodes of this transformation matrix are the periodically-stationary eigenmodes (Bloch-Floquet-Hill modes), and their eigenvalues determine the stability.

Without in any way minimizing the difficulties that are likely to be encountered in implementing these algorithms, the potential rewards are substantial — not only to provide insight to the intrinsic stability and noise level involved in nano-scale saturable absorbers and modelocked laser devices, but also in general to developing further generations of modelocked lasers. Historically, the modelocked laser community has been better at analysis than at synthesis. We understand the behavior of our existing lasers, and we can even perform some optimization tasks. However, we lack computational tools that can be reliably used to design lasers in new operating regimes. Our goal is to change that.

References

[1] C. R. Giles and E. Desurvire, "Modeling erbium-doped fiber amplifiers," J. Lightwave Technol. **9**, 271–283 (1991).

[2] A. G. Fox and T. Li, "Resonant Modes in a Maser Interferometer," (1961).

[3] J. A. Fleck, "Ultrashort-Pulse Generation by Q-Switched Lasers," Physical Review B **1**, 84–100 (1970).

[4] A. E. Siegman, *Lasers* (University Science Books, 1986).

[5] M. E. Fermann, A. Galvanauskas, and G. Sucha, *Ultrafast Lasers: Technology and Applications* (CRC Press, 2002).

[6] F. X. Kärtner, *Few-Cycle Laser Pulse Generation and Its Applications* (Springer Science & Business Media, 2004).

[7] C.-J. Chen, P. K. A. Wai, and C. R. Menyuk, "Soliton fiber ring laser," Optics Letters **17**, 417 (1992).

[8] A. Kim, J. Kutz, and D. Muraki, "Pulse-train uniformity in optical fiber lasers passively mode-locked by nonlinear polarization rotation," IEEE Journal of Quantum Electronics **36**, 465–471 (2000).

[9] F. Ilday, J. Buckley, L. Kuznetsova, and F. Wise, "Generation of 36-femtosecond pulses from a ytterbium fiber laser," Optics Express **11**, 3550 (2003).

[10] E. Ding, E. Shlizerman, and J. N. Kutz, "Generalized Master Equation for High-Energy Passive Mode-Locking: The Sinusoidal Ginzburg–Landau Equation," IEEE Journal of Quantum Electronics **47**, 705–714 (2011).

[11] A. Chong, W. H. Renninger, and F. W. Wise, "Properties of normal-dispersion femtosecond fiber lasers," Journal of the Optical Society of America B **25**, 140 (2008).

[12] W. H. Renninger, A. Chong, and F. W. Wise, "Amplifier similaritons in a dispersion-mapped fiber laser [Invited]." Optics express **19**, 22496–501 (2011).

[13] M. Baumgartl, B. Ortaç, J. Limpert, and A. Tünnermann, "Impact of dispersion on pulse dynamics in chirped-pulse fiber lasers," Applied Physics B **107**, 263–274 (2012).

[14] L. C. Sinclair, I. Coddington, W. C. Swann, G. B. Rieker, A. Hati, K. Iwakuni, and N. R. Newbury, "Operation of an optically coherent frequency comb outside the metrology lab," Optics Express **22**, 6996–7006 (2014).

[15] D. Popa, Z. Sun, T. Hasan, W. B. Cho, F. Wang, F. Torrisi, and a. C. Ferrari, "74-fs Nanotube-Mode-Locked Fiber Laser," Applied Physics Letters **101**, 17–19 (2012).

[16] S. Husaini and R. G. Bedford, "Graphene saturable absorber for high power semiconductor disk laser mode-locking," Applied Physics Letters **104**, 161107 (2014).

[17] E. Avrutin, J. Marsh, and E. Portnoi, "Monolithic and multi-gigahertz mode-locked semiconductor lasers: constructions, experiments, models and applications," Optoelectronics, IEE Proceedings **147**, 251–278 (2000).

[18] E. U. Rafailov, M. A. Cataluna, and W. Sibbett, "Mode-locked quantum-dot lasers," Nature Photonics **1**, 395–401 (2007).

[19] C. Saraceno, C. Schriber, M. Mangold, M. Hoffmann, O. Heckl, C. Baer, M. Golling, T. Südmeyer, and U. Keller, "SESAMs for

high-power oscillators: Design guidelines and damage thresholds," IEEE Journal of Selected Topics in Quantum Electronics **18**, 29–41 (2012).

[20] A. Martinez and Z. Sun, "Nanotube and graphene saturable absorbers for fibre lasers," Nature Photonics **7**, 842–845 (2013).

[21] J. N. Kutz, B. C. Collings, K. Bergman, S. Tsuda, S. T. Cundiff, W. H. Knox, P. Holmes, and M. Weinstein, "Mode-locking pulse dynamics in a fiber laser with a saturable Bragg reflector," Journal of the Optical Society of America B **14**, 2681 (1997).

[22] A. Cabasse, G. Martel, and J. L. Oudar, "High power dissipative soliton in an Erbium-doped fiber laser mode-locked with a high modulation depth saturable absorber mirror," Optics Express **17**, 9537 (2009).

[23] I. P. Christov and V. D. Stoev, "Kerr-lens mode-locked laser model: role of space time effects," Journal of the Optical Society of America B **15**, 1960 (1998).

[24] M. Y. Sander, J. Birge, A. Benedick, H. M. Crespo, and F. X. Kärtner, "Dynamics of dispersion managed octave-spanning titanium:sapphire lasers," Journal of the Optical Society of America B **26**, 743 (2009).

[25] W. H. Renninger and F. W. Wise, "Spatiotemporal soliton laser," Optica **1**, 101 (2014).

[26] J. N. Kutz, "Mode-locked soliton lasers," SIAM Review **48**, 629–678 (2006).

[27] N. Akhmediev and A. Ankiewicz, *Dissipative Solitons* (Springer Science & Business Media, 2005).

[28] N. Akhmediev and A. Ankiewicz, *Dissipative Solitons: From Optics to Biology and Medicine* (Springer, 2008).

[29] H. A. Haus, "Mode-locking of lasers," IEEE Journal on Selected Topics in Quantum Electronics **6**, 1173–1185 (2000).

[30] O. E. Martinez, R. L. Fork, and J. P. Gordon, "Theory of passively mode-locked lasers for the case of a nonlinear complex-propagation coefficient," Journal of the Optical Society of America B **2**, 753 (1985).

[31] H. A. Haus, "Theory of mode locking with a fast saturable absorber," Journal of Applied Physics **46**, 3049 (1975).

[32] C. C. Lee and T. R. Schibli, "Intrinsic power oscillations generated by the backaction of continuum on solitons and its implications on the transfer functions of a mode-locked laser," Phys. Rev. Lett. **112**, 223903 (2014).

[33] G. Biondini, "The dispersion-managed ginzburg–landau equation and its application to femtosecond lasers," Nonlinearity **21**, 2849 (2008).

[34] J. D. Moores, "On the Ginzburg-Landau laser mode-locking model with fifth-order saturable absorber term," Optics Communications **96**, 65–70 (1993).

[35] J. M. Soto-Crespo, N. N. Akhmediev, and V. V. Afanasjev, "Stability of the pulselike solutions of the quintic complex Ginzburg–Landau equation," Journal of the Optical Society of America B **13**, 1439 (1996).

[36] T. Kapitula, J. N. Kutz, and B. Sandstede, "Stability of pulses in the master mode-locking equation," Journal of the Optical Society of America B **19**, 740 (2002).

[37] J. M. Soto-Crespo, N. N. Akhmediev, V. V. Afanasjev, and S. Wabnitz, "Pulse solutions of the cubic-quintic complex Ginzburg-Landau equation in the case of normal dispersion," Physical Review E **55**, 4783–4796 (1997).

[38] N. Akhmediev, J. Soto-Crespo, and P. Grelu, "Roadmap to ultra-short record high-energy pulses out of laser oscillators," Physics Letters A **372**, 3124–3128 (2008).

[39] H. Leblond, M. Salhi, A. Hideur, T. Chartier, M. Brunel, and F. Sanchez, "Experimental and theoretical study of the passively mode-locked ytterbium-doped double-clad fiber laser," Physical Review A **65**, 063811 (2002).

[40] M. J. Ablowitz, T. P. Horikis, and B. Ilan, "Solitons in dispersion-managed mode-locked lasers," Physical Review A **77**, 033814 (2008).

[41] F. Kärtner, I. Jung, and U. Keller, "Soliton mode-locking with saturable absorbers," IEEE Journal of Selected Topics in Quantum Electronics **2**, 540–556 (1996).

[42] J. Proctor and J. N. Kutz, "Nonlinear mode-coupling for passive mode-locking: application of waveguide arrays, dual-core fibers, and/or fiber arrays." Optics express **13**, 8933–50 (2005).

[43] R. Paschotta, "Noise of mode-locked lasers (Part I): numerical model," Applied Physics B **79**, 153–162 (2004).

[44] R. Paschotta, "Noise of mode-locked lasers (Part II): timing jitter and other fluctuations," Applied Physics B **79**, 163–173 (2004).

[45] H. A. Haus and A. Mecozzi, "Noise of mode-locked lasers," IEEE Journal of Quantum Electronics **29**, 983–996 (1993).

[46] C. Antonelli, J. Chen, and F. X. Kärtner, "Intracavity pulse dynamics and stability for passively mode-locked lasers," Optics Express **15**, 5919 (2007).

[47] B. G. Bale and J. N. Kutz, "Variational method for mode-locked lasers," Journal of the Optical Society of America B **25**, 1193 (2008).

[48] B. R. Washburn, W. C. Swann, and N. R. Newbury, "Response dynamics of the frequency comb output from a femtosecond fiber laser," Optics Express **13**, 10622 (2005).

[49] N. Newbury and B. Washburn, "Theory of the frequency comb output from a femtosecond fiber laser," IEEE Journal of Quantum Electronics **41**, 1388–1402 (2005).

[50] F. Li, P. K. A. Wai, and J. N. Kutz, "Geometrical description of the onset of multi-pulsing in mode-locked laser cavities," Journal of the Optical Society of America B **27**, 2068 (2010).

[51] S. Namiki, E. P. Ippen, H. A. Haus, and C. X. Yu, "Energy rate equations for mode-locked lasers," Journal of the Optical Society of America B **14**, 2099 (1997).

[52] P. Kuchment, *Floquet Theory for Partial Differential Equations*, Operator Theory: Advances and Applications (Birkhäuser Basel, 2012).

[53] S. H. Strogatz, *Nonlinear Dynamics and Chaos: With Applications to Physics, Biology, Chemistry, and Engineering* (Westview Press, 1994).

[54] M. W. Hirsch, S. Smale, and R. L. Devaney, *Differential Equations, Dynamical Systems, and an Introduction to Chaos* (Academic Press, 2013).

[55] J. C. Maxwell, *On the stability of the motion of Saturn's Rings* (Macmillan & Company, 1859).

[56] H. A. Haus, J. G. Fujimoto, and E. P. Ippen, "Structures for additive pulse mode locking," Journal of the Optical Society of America B **8**, 2068 (1991).

[57] H. Haus and M. Islam, "Theory of the soliton laser," IEEE Journal of Quantum Electronics **21**, 1172–1188 (1985).

[58] L. Jiang, M. Grein, H. Haus, and E. Ippen, "Noise of mode-locked semiconductor lasers," IEEE Journal of Selected Topics in Quantum Electronics **7**, 159–167 (2001).

[59] J. N. Kutz and B. Sandstede, "Theory of passive harmonic mode-locking using waveguide arrays," Optics Express **16**, 636 (2008).

[60] E. P. Ippen, H. A. Haus, and L. Y. Liu, "Additive pulse mode locking," Journal of the Optical Society of America B **6**, 1736 (1989).

[61] C. Jirauschek, U. Morgner, and F. X. Kärtner, "Variational analysis of spatio-temporal pulse dynamics in dispersive Kerr media," Journal of the Optical Society of America B **19**, 1716 (2002).

[62] S. Wang, A. Docherty, B. S. Marks, and C. R. Menyuk, "Boundary tracking algorithms for determining the stability of mode-locked pulses," Journal of the Optical Society of America B **31**, 2914 (2014).

[63] M. J. Ablowitz and H. Segur, *Solitons and the Inverse Scattering Transform* (SIAM, 2006).

[64] G. Helmberg, *Introduction to Spectral Theory in Hilbert Space* (American Elsevier Publishing Company, 1969).

[65] D. J. Kaup, "Perturbation theory for solitons in optical fibers," Physical Review A **42**, 5689–5694 (1990).

[66] A. Friedman, *Foundations of Modern Analysis*, Dover Books on Mathematics Series (Dover, 1970).

[67] S. Wang, C. R. Menyuk, L. Sinclair, I. Coddington, and N. R. Newbury, "Soliton Wake Instability in a SESAM Modelocked Fiber Laser," in "CLEO: 2014," (OSA, Washington, D.C., 2014), p. SW3E.4.

[68] J. P. Gordon and H. A. Haus, "Random walk of coherently amplified solitons in optical fiber transmission," Optics Letters **11**, 665 (1986).

[69] J. P. Gordon and L. F. Mollenauer, "Phase noise in photonic communications systems using linear amplifiers," Optics Letters **15**, 1351 (1990).

[70] R. Schmeissner, J. Roslund, C. Fabre, and N. Treps, "Spectral Noise Correlations of an Ultrafast Frequency Comb," Physical Review Letters **113**, 263906 (2014).

[71] J. P. Gordon, "Dispersive perturbations of solitons of the nonlinear Schrödinger equation," Journal of the Optical Society of America B **9**, 91 (1992).

[72] F. X. Kärtner, D. Kopf, and U. Keller, "Solitary-pulse stabilization and shortening in actively mode-locked lasers," Journal of the Optical Society of America B **12**, 486 (1995).

[73] M. Abramowitz and I. Stegun, *Handbook of Mathematical Functions: With Formulas, Graphs, and Mathematical Tables*, Applied mathematics series (Dover Publications, 1964).

[74] C. R. Menyuk, J. K. Wahlstrand, J. Willits, R. P. Smith, T. R. Schibli, and S. T. Cundiff, "Pulse dynamics in mode-locked lasers: relaxation oscillations and frequency pulling," Opt. Express **15**, 6677–6689 (2007).

[75] J. K. Wahlstrand, J. T. Willits, C. R. Menyuk, and S. T. Cundiff, "The quantum-limited comb lineshape of a mode-locked laser: Fundamental limits on frequency uncertainty," Opt. Express **16**, 18624–18630 (2008).

[76] J. Nijhof, W. Forysiak, and N. Doran, "The averaging method for finding exactly periodic dispersion-managed solitons," IEEE Journal of Selected Topics in Quantum Electronics **6**, 330–336 (2000).

[77] R. Holzlohner, V. Grigoryan, C. Menyuk, and W. Kath, "Accurate calculation of eye diagrams and bit error rates in optical transmission systems using linearization," Journal of Lightwave Technology **20**, 389–400 (2002).

[78] B. Deconinck and J. Nathan Kutz, "Computing spectra of linear operators using the Floquet–Fourier–Hill method," Journal of Computational Physics **219**, 296–321 (2006).